EUROPEAN ORGANIZATION FOR NUCLEAR RESEARCH

CERN-PPE/92-174

14 October 1992

A Measurement of B Meson Production and Lifetime Using $D\ell^-$ Events in Z^0 Decays.

DELPHI Collaboration

Abstract

A study of B meson decays into $D\ell^-X$ final states is presented. In these events, neutral and charged D mesons originate predominantly from B^+ and B^0 decays, respectively. The dilution of this correlation due to D^{**} production has been taken into account. From 263700 hadronic Z^0 decays collected in 1991 with the DELPHI detector at the LEP collider, 92 $D^0 \to K^-\pi^+$, 35 $D^+ \to K^-\pi^+\pi^+$ and 61 $D^{*+} \to D^0\pi^+$ followed by $D^0 \to K^-\pi^+$ or $D^0 \to K^-\pi^+\pi^+\pi^-$, are found with an associated lepton of the same charge as the kaon. From the $D^0\ell^-$ and $D^{*+}\ell^-$, the probability f_d that a b quark hadronizes into a B^- (or $\bar{B}^0$) meson is found to be $0.44\pm0.08\pm0.09$, corresponding to a total $(B_s + \Lambda_b)$ hadronization fraction of $0.12^{+0.24}_{-0.12}$. By reconstructing the energy of each B meson, the b quark fragmentation is directly measured for the first time. The mean value of the B meson energy fraction is : $< X_E(B) >= 0.695 \pm 0.015(stat.) \pm 0.029(syst.)$

Reconstructing D-lepton vertices, the following B lifetimes are measured :

$$\begin{aligned}
\tau(B) &= 1.27^{+0.22}_{-0.18}(stat.) \pm 0.15(syst.) \text{ ps where } \bar{B} \to D^0\ell^-X \\
\tau(B) &= 1.18^{+0.39}_{-0.27}(stat.) \pm 0.15(syst.) \text{ ps where } \bar{B} \to D^+\ell^-X \\
\tau(B) &= 1.19^{+0.25}_{-0.19}(stat.) \pm 0.15(syst.) \text{ ps where } \bar{B} \to D^{*+}\ell^-X
\end{aligned}$$

and an average $\tau(B) = 1.23^{+0.14}_{-0.13}(stat.) \pm 0.15(syst.)$ ps is found. Allowing for decays into $D^{**}\ell^-\bar{\nu}$, the B^+ and B^0 lifetimes are :

$$\begin{aligned}
\tau(B^+) &= 1.30^{+0.33}_{-0.29}(stat.) \pm 0.15(syst.exp.) \pm 0.05(syst.D^{**}) \text{ ps} \\
\tau(B^0) &= 1.17^{+0.29}_{-0.23}(stat.) \pm 0.15(syst.exp.) \pm 0.05(syst.D^{**}) \text{ ps} \\
\tau(B^+)/\tau(B^0) &= 1.11^{+0.51}_{-0.39}(stat.) \pm 0.05(syst.exp.) \pm 0.10(syst.D^{**})
\end{aligned}$$

(Submitted to Zeit. Phys. C)

P.Abreu[20], W.Adam[48], T.Adye[36], E.Agasi[30], G.D.Alekseev[14], A.Algeri[13], P.Allen[47], S.Almehed[23], S.J.Alvsvaag[4], U.Amaldi[7], E.G.Anassontzis[3], A.Andreazza[27], P.Antilogus[24], W-D.Apel[15], R.J.Apsimon[36], B.Åsman[43], J-E.Augustin[18], A.Augustinus[30], P.Baillon[7], P.Bambade[18], F.Barao[20], R.Barate[12], G.Barbiellini[45], D.Y.Bardin[14], G.Barker[33], A.Baroncelli[39], O.Barring[23], J.A.Barrio[25], W.Bartl[48], M.J.Bates[36], M.Battaglia[13], M.Baubillier[22], K-H.Becks[50], C.J.Beeston[33], M.Begalli[35], P.Beilliere[6], Yu.Belokopytov[41], P.Beltran[9], D.Benedic[8], A.C.Benvenuti[5], M.Berggren[18], D.Bertrand[2], F.Bianchi[44], M.S.Bilenky[14], P.Billoir[22], J.Bjarne[23], D.Bloch[8], S.Blyth[33], V.Bocci[37], P.N.Bogolubov[14], T.Bolognese[38], M.Bonesini[27], W.Bonivento[27], P.S.L.Booth[21], P.Borgeaud[38], G.Borisov[41], H.Borner[7], C.Bosio[39], B.Bostjancic[42], S.Bosworth[33], O.Botner[46], B.Bouquet[18], C.Bourdarios[18], T.J.V.Bowcock[21], M.Bozzo[11], S.Braibant[2], P.Branchini[39], K.D.Brand[34], R.A.Brenner[7], H.Briand[22], C.Bricman[2], R.C.A.Brown[7], N.Brummer[30], J-M.Brunet[6], L.Bugge[32], T.Buran[32], H.Burmeister[7], J.A.M.A.Buytaert[7], M.Caccia[7], M.Calvi[27], A.J.Camacho Rozas[40], R.Campion[21], T.Camporesi[7], V.Canale[37], F.Cao[2], F.Carena[7], L.Carroll[21], C.Caso[11], M.V.Castillo Gimenez[47], A.Cattai[7], F.R.Cavallo[5], L.Cerrito[37], V.Chabaud[7], A.Chan[1], Ph.Charpentier[7], L.Chaussard[18], J.Chauveau[22], P.Checchia[34], G.A.Chelkov[14], L.Chevalier[38], P.Chliapnikov[41], V.Chorowicz[22], J.T.M.Chrin[47], M.P.Clara[44], P.Collins[33], J.L.Contreras[25], R.Contri[11], E.Cortina[47], G.Cosme[18], F.Couchot[18], H.B.Crawley[1], D.Crennell[36], G.Crosetti[11], M.Crozon[6], J.Cuevas Maestro[40], S.Czellar[13], E.Dahl-Jensen[28], B.Dalmagne[18], M.Dam[32], G.Damgaard[28], G.Darbo[11], E.Daubie[2], A.Daum[15], P.D.Dauncey[33], M.Davenport[7], P.David[22], J.Davies[21], W.Da Silva[22], C.Defoix[6], D.Delikaris[7], S.Delorme[7], P.Delpierre[6], N.Demaria[44], A.De Angelis[45], M.De Beer[38], H.De Boeck[2], W.De Boer[15], C.De Clercq[2], M.D.M.De Fez Laso[47], N.De Groot[30], C.De La Vaissiere[22], B.De Lotto[45], A.De Min[27], H.Dijkstra[7], L.Di Ciaccio[37], F.Djama[8], J.Dolbeau[6], M.Donszelmann[7], K.Doroba[49], M.Dracos[7], J.Drees[50], M.Dris[31], Y.Dufour[6], L-O.Eek[46], P.A.-M.Eerola[7], R.Ehret[15], T.Ekelof[46], G.Ekspong[43], A.Elliot Peisert[34], J-P.Engel[8], N.Ershaidat[22], D.Fassouliotis[31], M.Feindt[7], M.Fernandez Alonso[40], A.Ferrer[47], T.A.Filippas[31], A.Firestone[1], H.Foeth[7], E.Fokitis[31], F.Fontanelli[11], K.A.J.Forbes[21], J-L.Fousset[26], S.Francon[24], B.Franek[36], P.Frenkiel[6], D.C.Fries[15], A.G.Frodesen[4], R.Fruhwirth[48], F.Fulda-Quenzer[18], K.Furnival[21], H.Furstenau[15], J.Fuster[7], G.Galeazzi[34], D.Gamba[44], C.Garcia[47], J.Garcia[40], C.Gaspar[7], U.Gasparini[34], Ph.Gavillet[7], E.N.Gazis[31], J-P.Gerber[8], P.Giacomelli[7], R.Gokieli[49], B.Golob[42], V.M.Golovatyuk[14], J.J.Gomez Y Cadenas[7], A.Goobar[43], G.Gopal[36], M.Gorski[49], V.Gracco[11], A.Grant[7], F.Grard[2], E.Graziani[39], G.Grosdidier[18], E.Gross[7], P.Grosse-Wiesmann[7], B.Grossetete[22], S.Gumenyuk[41], J.Guy[36], U.Haedinger[15], F.Hahn[50], M.Hahn[15], S.Haider[30], A.Hakansson[23], A.Hallgren[46], K.Hamacher[50], G.Hamel De Monchenault[38], W.Hao[30], F.J.Harris[33], T.Henkes[7], J.J.Hernandez[47], P.Herquet[2], H.Herr[7], T.L.Hessing[21], I.Hietanen[13], C.O.Higgins[21], E.Higon[47], H.J.Hilke[7], S.D.Hodgson[33], T.Hofmokl[49], R.Holmes[1], S-O.Holmgren[43], D.Holthuizen[30], P.F.Honore[6], J.E.Hooper[28], M.Houlden[21], J.Hrubec[48], K.Huet[2], P.O.Hulth[43], K.Hultqvist[43], P.Ioannou[3], D.Isenhower[7], P-S.Iversen[4], J.N.Jackson[21], P.Jalocha[16], G.Jarlskog[23], P.Jarry[38], B.Jean-Marie[18], E.K.Johansson[43], D.Johnson[21], M.Jonker[7], L.Jonsson[23], P.Juillot[8], G.Kalkanis[3], G.Kalmus[36], F.Kapusta[22], M.Karlsson[7], E.Karvelas[9], S.Katsanevas[3], E.C.Katsoufis[31], R.Keranen[13], J.Kesteman[2], B.A.Khomenko[14], N.N.Khovanski[14], B.King[21], N.J.Kjaer[7], H.Klein[7], W.Klempt[7], A.Klovning[4], P.Kluit[30], A.Koch-Mehrin[50], J.H.Koehne[15], B.Koene[30], P.Kokkinias[9], M.Kopf[15], K.Korcyl[16], A.V.Korytov[14], V.Kostioukhine[41], C.Kourkoumelis[3], O.Kouznetsov[14], P.H.Kramer[50], J.Krolikowski[49], I.Kronkvist[23], U.Kruener-Marquis[50], W.Krupinski[16], K.Kulka[46], K.Kurvinen[13], C.Lacasta[47], C.Lambropoulos[9], J.W.Lamsa[1], L.Lanceri[45], V.Lapin[41], J-P.Laugier[38], R.Lauhakangas[13], G.Leder[48], F.Ledroit[12], R.Leitner[29], Y.Lemoigne[38], J.Lemonne[2], G.Lenzen[50], V.Lepeltier[18], T.Lesiak[16], J.M.Levy[8], E.Lieb[50], D.Liko[48], J.Lindgren[13], R.Lindner[50], A.Lipniacka[49], I.Lippi[34], B.Loerstad[23], M.Lokajicek[14], J.G.Loken[33], A.Lopez-Fernandez[7], M.A.Lopez Aguera[40], M.Los[30], D.Loukas[9], J.J.Lozano[47], P.Lutz[6], L.Lyons[33], G.Maehlum[32], J.Maillard[6], A.Maltezos[9], F.Mandl[48], J.Marco[40], M.Margoni[34], J-C.Marin[7], A.Markou[9], T.Maron[50], S.Marti[47], L.Mathis[1], F.Matorras[40], C.Matteuzzi[27], G.Matthiae[37], M.Mazzucato[34], M.Mc Cubbin[21], R.Mc Kay[1], R.Mc Nulty[21], G.Meola[11], C.Meroni[27], W.T.Meyer[1], M.Michelotto[34], I.Mikulec[48], L.Mirabito[24], W.A.Mitaroff[48], G.V.Mitselmakher[14], U.Mjoernmark[23], T.Moa[43], R.Moeller[28], K.Moenig[7], M.R.Monge[11], P.Morettini[11], H.Mueller[15], W.J.Murray[36], B.Muryn[16], G.Myatt[33], F.L.Navarria[5], P.Negri[27], B.S.Nielsen[28], B.Nijjhar[21], V.Nikolaenko[41], P.E.S.Nilsen[4], P.Niss[43], V.Obraztsov[41], A.G.Olshevski[14], R.Orava[13], A.Ostankov[41], K.Osterberg[13], A.Ouraou[38], M.Paganoni[27], R.Pain[22], H.Palka[30], Th.D.Papadopoulou[31], L.Pape[7], A.Passeri[39], M.Pegoraro[34], J.Pennanen[13], V.Perevozchikov[41], M.Pernicka[48], A.Perrotta[5], C.Petridou[45], A.Petrolini[11], L.Petrovykh[41], T.E.Pettersen[34], F.Pierre[38], M.Pimenta[20], O.Pingot[2], S.Plaszczynski[18], M.E.Pol[7], G.Polok[16], P.Poropat[45], P.Privitera[15], A.Pullia[27], D.Radojicic[33], S.Ragazzi[27], H.Rahmani[31], P.N.Ratoff[19], A.L.Read[32], N.G.Redaelli[27], M.Regler[48], D.Reid[21], P.B.Renton[33], L.K.Resvanis[3], F.Richard[18], M.Richardson[21], J.Ridky[10], G.Rinaudo[44], I.Roditi[17], A.Romero[44], I.Roncagliolo[11], P.Ronchese[34], C.Ronnqvist[13], E.I.Rosenberg[1], S.Rossi[7], U.Rossi[5], E.Rosso[7], P.Roudeau[18], T.Rovelli[5], W.Ruckstuhl[30], V.Ruhlmann-Kleider[38], A.Ruiz[40], K.Rybicki[16], H.Saarikko[13], Y.Sacquin[38], G.Sajot[12], J.Salt[47], J.Sanchez[25], M.Sannino[11], S.Schael[15], H.Schneider[15], B.Schulze[37], M.A.E.Schyns[50], G.Sciolla[44], F.Scuri[45], A.M.Segar[33], R.Sekulin[36], M.Sessa[45], G.Sette[11], R.Seufert[15],

R.C.Shellard[35], I.Siccama[30], P.Siegrist[38], S.Simonetti[11], F.Simonetto[34], A.N.Sisakian[14], T.B.Skaali[32], G.Skjevling[32], G.Smadja[38,24], G.R.Smith[36], R.Sosnowski[7], T.S.Spassoff[12], E.Spiriti[39], S.Squarcia[11], H.Staeck[50], C.Stanescu[39], S.Stapnes[32], G.Stavropoulos[9], F.Stichelbaut[2], A.Stocchi[18], J.Strauss[48], J.Straver[7], R.Strub[8], M.Szczekowski[7], M.Szeptycka[49], P.Szymanski[49], T.Tabarelli[27], S.Tavernier[2], O.Tchikilev[41], G.E.Theodosiou[9], A.Tilquin[26], J.Timmermans[30], V.G.Timofeev[14], L.G.Tkatchev[14], T.Todorov[8], D.Z.Toet[30], O.Toker[13], E.Torassa[44], L.Tortora[39], D.Treille[7], U.Trevisan[11], W.Trischuk[7], G.Tristram[6], C.Troncon[27], A.Tsirou[7], E.N.Tsyganov[14], M.Turala[16], M-L.Turluer[38], T.Tuuva[13], I.A.Tyapkin[22], M.Tyndel[36], S.Tzamarias[7], S.Ueberschaer[50], O.Ullaland[7], V.Uvarov[41], G.Valenti[5], E.Vallazza[44], J.A.Valls Ferrer[47], C.Vander Velde[2], G.W.Van Apeldoorn[30], P.Van Dam[30], M.Van Der Heijden[30], W.K.Van Doninck[2], P.Vaz[7], G.Vegni[27], L.Ventura[34], W.Venus[36], F.Verbeure[2], L.S.Vertogradov[14], D.Vilanova[38], P.Vincent[24], L.Vitale[13], E.Vlasov[41], A.S.Vodopyanov[14], M.Vollmer[50], G.Voulgaris[3], M.Voutilainen[13], V.Vrba[39], H.Wahlen[50], C.Walck[43], F.Waldner[45], M.Wayne[1], A.Wehr[50], M.Weierstall[50], P.Weilhammer[7], J.Werner[50], A.M.Wetherell[7], J.H.Wickens[2], J.Wikne[32], G.R.Wilkinson[33], W.S.C.Williams[33], M.Winter[8], M.Witek[16], D.Wormald[32], G.Wormser[18], K.Woschnagg[46], N.Yamdagni[43], P.Yepes[7], A.Zaitsev[41], A.Zalewska[16], P.Zalewski[18], D.Zavrtanik[42], E.Zevgolatakos[9], G.Zhang[50], N.I.Zimin[14], M.Zito[38], R.Zuberi[33], R.Zukanovich Funchal[6], G.Zumerle[34], J.Zuniga[47]

[1] Ames Laboratory and Department of Physics, Iowa State University, Ames IA 50011, USA
[2] Physics Department, Univ. Instelling Antwerpen, Universiteitsplein 1, B-2610 Wilrijk, Belgium
and IIHE, ULB-VUB, Pleinlaan 2, B-1050 Brussels, Belgium
and Faculté des Sciences, Univ. de l'Etat Mons, Av. Maistriau 19, B-7000 Mons, Belgium
[3] Physics Laboratory, University of Athens, Solonos Str. 104, GR-10680 Athens, Greece
[4] Department of Physics, University of Bergen, Allégaten 55, N-5007 Bergen, Norway
[5] Dipartimento di Fisica, Università di Bologna and INFN, Via Irnerio 46, I-40126 Bologna, Italy
[6] Collège de France, Lab. de Physique Corpusculaire, IN2P3-CNRS, F-75231 Paris Cedex 05, France
[7] CERN, CH-1211 Geneva 23, Switzerland
[8] Centre de Recherche Nucléaire, IN2P3 - CNRS/ULP - BP20, F-67037 Strasbourg Cedex, France
[9] Institute of Nuclear Physics, N.C.S.R. Demokritos, P.O. Box 60228, GR-15310 Athens, Greece
[10] FZU, Inst. of Physics of the C.A.S. High Energy Physics Division, Na Slovance 2, CS-180 40, Praha 8, Czechoslovakia
[11] Dipartimento di Fisica, Università di Genova and INFN, Via Dodecaneso 33, I-16146 Genova, Italy
[12] Institut des Sciences Nucléaires, IN2P3-CNRS, Université de Grenoble 1, F-38026 Grenoble, France
[13] Research Institute for High Energy Physics, SEFT, Siltavuorenpenger 20 C, SF-00170 Helsinki, Finland
[14] Joint Institute for Nuclear Research, Dubna, Head Post Office, P.O. Box 79, 101 000 Moscow, USSR.
[15] Institut für Experimentelle Kernphysik, Universität Karlsruhe, Postfach 6980, D-7500 Karlsruhe 1, FRG
[16] High Energy Physics Laboratory, Institute of Nuclear Physics, Ul. Kawiory 26 a, PL-30055 Krakow 30, Poland
[17] Centro Brasileiro de Pesquisas Físicas, rua Xavier Sigaud 150, RJ-22290 Rio de Janeiro, Brazil
[18] Université de Paris-Sud, Lab. de l'Accélérateur Linéaire, IN2P3-CNRS, Bat 200, F-91405 Orsay, France
[19] School of Physics and Materials, University of Lancaster - Lancaster LA1 4YB, UK
[20] LIP, IST, FOUL - Av. Elias Garcia, 14 - 1°, P-1000 Lisboa Codex, Portugal
[21] Department of Physics, University of Liverpool, P.O. Box 147, GB - Liverpool L69 3BX, UK
[22] LPNHE, IN2P3-CNRS, Universités Paris VI et VII, Tour 33 (RdC), 4 place Jussieu, F-75230 Paris Cedex 05, France
[23] Department of Physics, University of Lund, Sölvegatan 14, S-22363 Lund, Sweden
[24] Université Claude Bernard de Lyon, IPNL, IN2P3-CNRS, F-69622 Villeurbanne Cedex, France
[25] Universidad Complutense, Avda. Complutense s/n, E-28040 Madrid, Spain
[26] Univ. d'Aix - Marseille II - CPP, IN2P3-CNRS, F-13288 Marseille Cedex 09, France
[27] Dipartimento di Fisica, Università di Milano and INFN, Via Celoria 16, I-20133 Milan, Italy
[28] Niels Bohr Institute, Blegdamsvej 17, DK-2100 Copenhagen 0, Denmark
[29] NC, Nuclear Centre of MFF, Charles University, Areal MFF, V Holesovickach 2, CS-180 00, Praha 8, Czechoslovakia
[30] NIKHEF-H, Postbus 41882, NL-1009 DB Amsterdam, The Netherlands
[31] National Technical University, Physics Department, Zografou Campus, GR-15773 Athens, Greece
[32] Physics Department, University of Oslo, Blindern, N-1000 Oslo 3, Norway
[33] Nuclear Physics Laboratory, University of Oxford, Keble Road, GB - Oxford OX1 3RH, UK
[34] Dipartimento di Fisica, Università di Padova and INFN, Via Marzolo 8, I-35131 Padua, Italy
[35] Depto. de Fisica, Pontificia Univ. Católica, C.P. 38071 RJ-22453 Rio de Janeiro, Brazil
[36] Rutherford Appleton Laboratory, Chilton, GB - Didcot OX11 OQX, UK
[37] Dipartimento di Fisica, Università di Roma II and INFN, Tor Vergata, I-00173 Rome, Italy
[38] Centre d'Etude de Saclay, DSM/DAPNIA, F-91191 Gif-sur-Yvette Cedex, France
[39] Istituto Superiore di Sanità, Ist. Naz. di Fisica Nucl. (INFN), Viale Regina Elena 299, I-00161 Rome, Italy
[40] Facultad de Ciencias, Universidad de Santander, av. de los Castros, E - 39005 Santander, Spain
[41] Inst. for High Energy Physics, Serpukow P.O. Box 35, Protvino, (Moscow Region), CEI
[42] Institut "Jozef Stefan", Ljubljana, Slovenija
[43] Institute of Physics, University of Stockholm, Vanadisvägen 9, S-113 46 Stockholm, Sweden
[44] Dipartimento di Fisica Sperimentale, Università di Torino and INFN, Via P. Giuria 1, I-10125 Turin, Italy
[45] Dipartimento di Fisica, Università di Trieste and INFN, Via A. Valerio 2, I-34127 Trieste, Italy
and Istituto di Fisica, Università di Udine, I-33100 Udine, Italy
[46] Department of Radiation Sciences, University of Uppsala, P.O. Box 535, S-751 21 Uppsala, Sweden
[47] IFIC, Valencia-CSIC, and D.F.A.M.N., U. de Valencia, Avda. Dr. Moliner 50, E-46100 Burjassot (Valencia), Spain
[48] Institut für Hochenergiephysik, Österr. Akad. d. Wissensch., Nikolsdorfergasse 18, A-1050 Vienna, Austria
[49] Inst. Nuclear Studies and, University of Warsaw, Ul. Hoza 69, PL-00681 Warsaw, Poland
[50] Fachbereich Physik, University of Wuppertal, Postfach 100 127, D-5600 Wuppertal 1, FRG

1 Introduction

Many interesting topics concerning weak b-decays can be understood through a precise study of B meson semileptonic decays. Comparing the semileptonic branching fractions of the B particles checks the extent to which spectator graphs dominate [1]. In the pure spectator model and assuming that only D and D^* mesons are produced in B^0 and B^+ semileptonic decays [†] , all $D^+\ell^-$ or $D^{*+}\ell^-$ pairs should originate from $\bar{B}^0$ mesons and all $D^0\ell^-$ pairs, where the D^0 is not from a D^{*+} decay, should come from B^- mesons. Although this correlation is diluted by the production of D^{**} mesons, enough remains to allow the determination of the B^0 and B^+ lifetimes. Compared to experiments at the $\Upsilon(4S)$ energy [2] [3], where b-hadrons are produced almost at rest, it is possible to measure directly at LEP the neutral and charged B meson lifetimes, without relying on knowledge of the B decay partial widths and production rate at the $\Upsilon(4S)$ resonance. Finally, if both a D meson and a charged lepton are detected only the neutrino escapes detection, and it is possible to reconstruct the B energy and measure the b quark fragmentation function more directly than with the inclusive lepton spectrum.

All hadronic Z^0 decays collected in 1991 at LEP with the DELPHI detector are used. The analysis selects B decays into a D meson together with an identified lepton. The silicon strip Vertex Detector separates primary and secondary vertices and improves the momentum resolution of charged particles. Charmed mesons are reconstructed if an identified lepton is produced in the same direction ($\vec{p}(\ell^-) \cdot \vec{p}(K^-) > 0$) as any of the following decays :

- $D^0 \to K^-\pi^+$
- $D^+ \to K^-\pi^+\pi^+$
- $D^{*+} \to D^0\pi^+$ followed by $D^0 \to K^-\pi^+$ or $D^0 \to K^-\pi^+\pi^+\pi^-$

where the kaon candidate is required to have the same charge as the lepton.

The criteria for selecting hadronic Z^0 events and for identifying leptons are explained in section 2. The vertex reconstructions and selections made for the different decays are detailed in section 3. The measurement of the branching fractions of $\bar{B}$ mesons into $D\ell^-X$ final states are given in section 4, the probability f_d that a b quark hadronizes into a $\bar{B}^0$ meson is evaluated and the yield of B particles other than B^0 and B^+ is given. By estimating the original B momentum, the b quark fragmentation function is shown in section 5 and compared to previous measurements. Reconstructing the B decay length as the distance from production to the D-lepton vertex, the B meson lifetime is presented in section 6 for each individual $D\ell^-X$ channel. Finally, taking into account B decays into $D^{**}\ell^-\bar{\nu}$, the B^+ and B^0 lifetimes are given in section 7.

2 Detector description and event selection

A description of the DELPHI apparatus can be found in reference [4]. The Vertex Detector (VD) consisted in 1991 of three layers of silicon, at radii 6.5 cm, 9 cm and 11 cm. They measure Rϕ coordinates over a length of 24 cm, and define an angular acceptance of 27-153^0, 37-143^0 and 42-138^0 for hits in one, two or three layers. The absolute hit resolution in the plane transverse to the beam axis has been measured to be 8.0 μm . The TPC, the principal tracking device of DELPHI, is a cylinder of 30 cm inner radius, 122 cm outer radius and has a length of 2.7 m. Each end-cap is divided into 6 sector plates each with 192 sense wires used for the particle identification. The dE/dx energy

[†] Throughout the paper the notation B^0 refers uniquely to the B_d^0 meson, and charge-conjugate states are implicitly included.

loss of a charged particle is measured by these wires as the 80% truncated mean of the maximum amplitudes of the wire signals. For particles in hadronic jets, the resolution has been measured to be 7.5%. However 25% of the tracks have no information because they are too close to another track or have too few wire hits (a minimum of 30 wires was required). The dE/dx spectra measured for kaons and pions are shown on Figure 1-a, where the two samples have been selected using the Cherenkov counter RICH [5] for momenta between 8 and 15 GeV/c. The unhatched histogram shows the difference between the measured ionization for the kaon enriched sample and the one expected for a kaon. The hatched histogram shows the same quantity for the pion enriched sample. The dE/dx measurement thus allows some separation of K from π.

Charged particles were reconstructed with the tracking detectors and with the associated VD hits. The momentum resolution was found to be 3.5% for 45 GeV/c muons and is proportional to the momentum. The charged particles were retained if they satisfied the following selection criteria :

- momentum between 0.4 and 50 GeV/c;
- relative error on momentum measurement less than 100%;
- over 30 cm track length in the TPC;
- projection of impact parameter relative to the interaction point below 4 cm in the plane transverse to the beam direction;
- distance to the nominal interaction point along the beam direction below 10 cm.

These selections allow a reliable measurement of the multiplicity and momentum of the charged particles. Neutral particles were reconstructed from energy deposits in calorimeters which were not associated to a measured charged particle. Hadronic events were then accepted by requiring :

- 5 or more charged particles;
- total energy of the charged particles larger than 12% of the centre-of-mass energy, assuming all charged particles to be pions.

The hadronic decay selection efficiency was found to be 95.0±0.5% . A total of 250500 hadronic events was selected from the 1991 data, corresponding to 263700 collected Z^0.

Events with lepton candidates were selected as described in detail in a recent paper[6]. Both muons and electrons were used. The muon selection was the same as in reference [6] with a minimum momentum of 3 GeV/c and has an efficiency of 77±5%. For electrons, in order to enhance the efficiency, looser selections were used than those in reference [6]. The minimum momentum was 3 GeV/c and the efficiency was 64±5%.

Charged particles were associated to jets by using the LUCLUS algorithm with default parameter [7]. For the jet containing the lepton candidate, the jet axis was defined as the sum of the momenta of all charged particles belonging to this jet not including the lepton. When a p_T cut is applied, p_T is defined as the transverse momentum of the lepton with respect to this jet axis.

3 Charmed meson reconstruction

The analysis of charmed mesons is based mainly on the separation of primary and secondary vertices. The beam spot constraint is added into a primary vertex fit by using the mean transverse position of the beam known for each fill. The measured widths of the beam spot are 150 μm in the horizontal and 10 μm in the vertical directions.

For the complete reconstruction of charmed mesons, only charged particles produced in the same direction as the lepton were considered ($\vec{p}(\ell^-) \cdot \vec{p} > 0$). In this case the

combinatorial background is smaller because of the reduced mean charged multiplicity observed in B semileptonic decays. The kaon candidate in D decay was required to have the same charge as the identified lepton. In the $D^0 \to K^-\pi^+\pi^+\pi^-$ case, the kaon mass was assigned in turn to the particles of the same charge as the lepton. This decay mode was not used for the direct D^0 study because of the larger combinatorial background. Particle identification was only used to discriminate between kaon and pion in D^+ decays.

According to the D^0 or D^+ decay final states, a $K^-\pi^+$, $K^-\pi^+\pi^+$ or $K^-\pi^+\pi^+\pi^-$ combination was selected to compute a secondary vertex in space. At least two charged particles among these were required to have at least two hits associated in the Vertex Detector (except in the small region where only one hit is possible). The momentum vector of each particle was taken from this geometrical secondary vertex fit. The D^0, D^+ or D^{*+} meson was selected if its energy fraction $X_E(D)=E_D/E_{beam}$ was larger than 0.15.

3.1 $D^0 \to K^-\pi^+$ channel

The reduction of the combinatorial background under the $D^0 \to K^-\pi^+$ peak is based on two complementary methods. One uses the fact that in the selected decays of the B mesons, the apparent decay length of D^0 mesons is large (several millimetres) compared to the decay length resolution (typically 300μm). Therefore, the requirement of a detached secondary vertex reduces the combinatorial background significantly. The second increases the beauty fraction by requiring a transverse momentum p_T above 1 GeV/c for the lepton.

Charged particles were considered if they had momentum above 1.5 GeV/c. The transverse decay length, ΔL, is the distance in the Rϕ transverse plane between the primary and secondary vertices. This decay length was given the same sign as the scalar product of the pair momentum with the vector joining the primary to the secondary vertex.

Figure 2-a displays this decay length distribution for all combinations with an invariant mass above 1.5 GeV/c^2 . The width corresponds to a decay length resolution of 300 μm , including both primary vertex and secondary vertex resolutions, the latter dominating the total resolution. The clear asymmetry between negative and positive decay lengths is due to beauty and charm particle decays. Figure 2-b shows the normalised transverse decay length, $\Delta L/\sigma$, where the transverse decay length error, σ, is given by the vertex fit. The negative part of the distribution is well described by summing a Gaussian of unit width and a flat tail due to badly associated tracks.

The $K^-\pi^+$ invariant mass distribution obtained for combinations where $\Delta L/\sigma$ is greater than 1 is displayed in Figure 3. A fit was performed to extract the number of reconstructed D^0 with the background described by an exponential. The signal was the sum of two terms : a Gaussian at the observed D^0 peak and a second function describing the $K^-\pi^+$ mass spectrum originating from the decay $D^0 \to K^-\pi^+\pi^0$, as predicted by the simulation [7]. The $(K^-\pi^+\pi^0)/(K^-\pi^+)$ ratio was fixed to the Monte Carlo expectation of 1.8, which takes into account the relative branching fractions and the kinematics of the $K^-\pi^+\pi^0$ decay channel. The fit yields 92$\pm$14 D^0 decaying into $K^-\pi^+$. The width of the D^0 peak is 16$\pm$2 MeV/c^2 , in agreement with the Monte Carlo expectation, while the mean mass (1852$\pm$2 MeV/c^2) is 12 MeV/c^2 below the world average value [8]. This mass shift is attributed to residual alignment errors of the different detectors used in the tracking and to an imperfect correction for the energy lost in the material crossed by the particles before the detectors.

The D^0 candidates were selected if their invariant mass was in the range 1810−1890 MeV/c^2 . The background from the fit is 35±5%. The background energy spectrum was obtained from an average of two sources in order to take into account possible systematic bias : the wings of the mass peak (in the intervals 1.7−1.8 GeV/c^2 and 2.0−2.1 GeV/c^2) and the "K"π spectrum where the pseudo-kaon particle was incompatible with a real kaon according to the dE/dx measurement. The latter distribution has no contribution from real D mesons. The quality of the dE/dx measurement can be seen on Figure 1-b, where the difference between the observed dE/dx for the kaon track of the D^0 candidate and the expected kaon ionization loss is displayed. This agrees with the sample of kaons selected by the RICH (Fig. 1-a). Since pion and kaon ionization curves have the same momentum dependence, no significant bias is expected from this background selection.

The reconstruction efficiency, computed using the Monte Carlo simulation, was found to be almost constant over the D^0 energy range. The acceptance corrected $X_E(D)$=E_D/E_{beam} distribution is displayed in Figure 4. The solid line corresponds to the Monte Carlo prediction which includes 20% of D^{**} mesons from B decays. The b fragmentation function reproduces the inclusive lepton spectrum[6]. The observed $X_E(D)$ distribution is in agreement with the prediction, perhaps a little softer. The softness of the observed distribution supports the hypothesis that all these D^0 come from B decays, since D from primary charmed quarks should have a much harder $X_E(D)$ distribution.

Another check of the source of these D^0 mesons is their apparent proper time distribution. Those originating from charm will have a pure exponential distribution corresponding to the well known D^0 lifetime. Those originating from beauty will have a much flatter distribution. Figure 5 shows the observed distribution and the predictions assuming a pure charm source (solid line) and a pure beauty source (histogram) generated with a B meson lifetime of 1.2 ps. The distribution clearly indicates B mesons are the dominant source of these D^0.

3.2 $D^+ \to K^-\pi^+\pi^+$ channel

The $D^+ \to K^-\pi^+\pi^+$ decay was reconstructed in a similar way as the previous channel :

- A lepton with p_T above 1 GeV/c was asked for.
- The momenta of the kaon and pion candidates had to exceed 1.5 and 1 GeV/c, respectively.
- A secondary $K^-\pi^+\pi^+$ vertex was computed. The track combination was retained if the χ^2 probability was larger than 1% and if the apparent transverse decay length fulfilled $\Delta L/\sigma > 1.5$.
- However, due to the larger combinatorial background under the D^+ signal, the measured dE/dx of the kaon candidate was in addition required to be two standard deviations lower than the theoretical energy loss of a pion.

The contamination of the remaining sample by the decay chain $D^{*+} \to D^0\pi^+$ followed by $D^0 \to K^-\pi^+$ was eliminated by rejecting all combinations where $\Delta M = M(K^-\pi^+\pi^+) - M(K^-\pi^+)$ was less than 150 MeV/c^2 . The invariant mass distribution $K^-\pi^+\pi^+$ of the final sample is displayed in Figure 6 when associated to a lepton ℓ^- (solid line histogram) or ℓ^+ (hatched histogram). The $D^+\ell^-$ signal, 35±8 events, was determined by fitting a linear function for the background and a Gaussian for the D^+ peak. The fitted D^+ mass is 1862±3 MeV/c^2 , slightly lower than the expected value 1869.3±0.5 MeV/c^2 [8], and the width is 13±3 MeV/c^2 . No signal was observed in the wrong sign $D^+\ell^+$ sample. The D^+ candidates were selected for the B lifetime measure-

ment if their invariant mass was in the range 1830−1900 MeV/c^2 . The background was taken in the ranges 1600−1800 and 1940−2140 MeV/c^2 . Due to the lower production rate times branching fraction into $K^-K^+\pi^+$ final states, the D_s contamination in the background was estimated to be negligible .

3.3 $D^{*+} \to (K^-\pi^+)\pi^+$ or $(K^-\pi^+\pi^+\pi^-)\pi^+$ channels

The selection criteria for the decay $D^{*+} \to D^0\pi^+$ followed by $D^0 \to K^-\pi^+$ or $D^0 \to K^-\pi^+\pi^+\pi^-$ relied mainly on the peculiar kinematics of the pion from the D^{*+} decay, hereafter called the bachelor pion, and on the reconstruction of primary and secondary vertices.

Due to the different combinatorial backgrounds and kinematics, different selections on the momenta were used in the two channels : the K momentum had to exceed 1 GeV/c (2 GeV/c), while the π momentum had to exceed 1 GeV/c (0.4 GeV/c) in the $K\pi$ ($K3\pi$) modes.

To reduce the combinatorial background in the $K3\pi$ mode, the impact parameter of each track with respect to the secondary vertex was required to be less than 0.75 cm, the apparent transverse decay length had to fulfil $\Delta L/\sigma > 1$, and a lepton with p_T larger than 1 GeV/c was asked for.

To reduce the combinatorial background in the $K\pi$ mode, the angle θ^* between the D^0 flight direction and the kaon direction in the D^0 rest frame was required to satisfy $\cos\theta^* > -0.9$. For genuine D^0 candidates an isotropic distribution is expected whereas the background is strongly peaked in the backward direction.

The mass difference ΔM=M("D^0"π)-M("D^0") was computed by adding in turn all possible bachelor pions, where "D^0" refers here to candidate $K\pi$ or $K3\pi$ combinations without their mass being constrained to the D^0 mass. In order to reject poorly measured tracks, only charged particles with an impact parameter lower than 0.3 cm with respect to the primary vertex were retained as bachelor pion candidates. Their resolution was enhanced by taking their four-momentum after fitting to pass through the primary vertex. These requirements improve the ΔM resolution and the signal-to-noise ratio without loss of genuine D^{*+} from B decays. The bachelor pion momentum had to be between 0.3 and 4.5 GeV/c, corresponding to $0.15 < X_E(D^{*+}) < 1.0$.

The mass difference ΔM is shown in Figure 7 (a) and (b) for the $(K\pi)\pi$ and $(K3\pi)\pi$ modes. These distributions are given for a $(K\pi)$ or $(K3\pi)$ mass between 1820 and 1900 MeV/c^2 . The unhatched histogram is the $(K^-\ell^-)$ charge combinations and shows a clear signal for the $D^{*+}\ell^-$ associations, whereas the hatched histogram shows the wrong $(K^-\ell^+)$ combinations which do not give a D^{*+} signal.

The signal in the mass difference distribution was described by a Gaussian and the background by the function $\alpha(\Delta\text{M-}m_\pi)^\beta$ (curves in Figure 7). The number of $(D^{*+}\ell^-)$ events is 30±6 in the $(K\pi)$ mode and 31±10 in the $(K3\pi)$ mode, with a signal/background ratio of 4.7 and 1.3, respectively. The mean ΔM are 145.3±0.1 and 145.3±0.2 MeV/c^2 , respectively, in good agreement with the mass difference 145.44±0.06 MeV/c^2 between D^{*+} and D^0 mesons [8], and the resolution is 0.7 MeV/c^2 in both cases.

A particle combination was retained as a D^{*+} candidate if the $K\pi$ or the $K3\pi$ mass was in the range 1820−1900 MeV/c^2 and if the ΔM was between 143.5 and 147.5 MeV/c^2 .

4 Decay fraction of b quarks to $\bar{B}^0$ and B^-

Events in which a D^0 or a D^{*+} is produced in association with a lepton are largely dominated by $\bar{B}^0$ and B^- decays. Since these semileptonic decay rates have been measured by lower energy experiments at threshold [2] [9], the probability that a b quark produces a $\bar{B}^0$ or a B^- can be deduced. This measurement is interesting for two reasons : firstly, once the $\bar{B}^0$ and B^- production is known, then the total amount of $\bar{B}_s$ and Λ_b can be evaluated; secondly, the B^0 fraction is a key parameter in the interpretation of the mixing parameter χ.

When comparing LEP and $\Upsilon(4S)$ measurements, it is important to check that the production of B^* or B^{**} mesons that occur only at LEP does not bias the comparison. This would occur if the fractions of $\bar{B}^0$ and B^- production were affected by the production of these excited states, in a fashion similar to the charm case where the decay $D^{*0} \to D^+\pi^-$ is kinematically forbidden. However this is not the case for B decays, since B^* mesons decay into a B meson and a photon, and B^{**} mesons are estimated to lie far above the pion threshold [10].

The measurement proceeds as follows: let f_d (f_u) be the probability that a b quark produces a $\bar{B}^0$ (B^-) meson, and let $d_{\bar{B}^0}$ (d_{B^-}) be the D^0 meson yield in $\bar{B}^0$ (B^-) semileptonic decays. Neglecting at this stage the D^0 from $\bar{B}_s$ and Λ_b semileptonic decays, the fraction of b semileptonic decays containing a D^0 is :

$$P_{sl}(b \to D^0\ell^- X) = f_d d_{\bar{B}^0} + f_u d_{B^-} \tag{1}$$

The probabilities f_d and f_u are now assumed to be equal, because of the SU_2 isospin symmetry and because the mass difference between $\bar{B}^0$ and B^- mesons is small[11]. Hence :

$$P_{sl}(b \to D^0\ell^- X) = f_d(d_{\bar{B}^0} + d_{B^-}) \tag{2}$$

The term $(d_{\bar{B}^0} + d_{B^-})/2$ is the average inclusive D^0 yield in $\bar{B}$ semileptonic decays from the $\Upsilon(4S)$ and is $0.79 \pm 0.10 \pm 0.07$ for the D^0 [2] and $0.39 \pm 0.10 \pm 0.04$ for the D^{*+} [9] [12]. Furthermore, since D^0 and D^{*+} are used in the same decay channels as at low energy, all the branching fractions cancel in the comparison. The probability that a b quark produces a $\bar{B}^0$ (or B^-) meson is :

$$f_d = \frac{1}{2} \cdot \frac{P_{LEP}(b \to D^0\ell^- X)}{P_{\Upsilon(4S)}(B \to D^0\ell^- X)} \tag{3}$$

The same formula holds true for the D^{*+} production, so in practice the two measurements can be combined. Thus the relative inclusive D^0 and D^{*+} production in b semileptonic decays should be the same at LEP and at the $\Upsilon(4S)$ resonance.

The acceptance times the efficiencies is 12% for the $D^0\ell^-$ with lepton p_T above 1 GeV/c where $D^0 \to K^-\pi^+$, and 15% for the $D^{*+}\ell^-$ where $D^{*+} \to (K^-\pi^+)\pi^+$. The contribution from $D^{*+}\bar{D}X$ production followed by a semileptonic decay of the $\bar{D}$ daughter is estimated from the Monte Carlo simulation [7] to be $14 \pm 5\%$ of the generated $\bar{B}^0 \to D^{*+}\ell^- X$ events. This proportion of events was subtracted from the $D^{*+}\ell^-$ sample. In the $D^0\ell^-$ sample, the requirement that the lepton p_T is above 1 GeV/c avoids the similar contribution from $D^0\bar{D}X$. Using the branching fraction $\Gamma_b/\Gamma_{had} \cdot Br(b \to \ell^- X) = 0.0238 \pm 0.0004(stat.) \pm 0.0012(syst.)$ as measured at LEP [6] [13], the fraction of b semileptonic decays containing a D^0 or D^{*+} is :

$$\begin{aligned} P_{sl}(b \to D^0\ell^- X) &= 0.84 \pm 0.13 \pm 0.17 \\ P_{sl}(b \to D^{*+}\ell^- X) &= 0.28 \pm 0.06 \pm 0.06 \end{aligned}$$

from which the following results can be derived :

(i) $P_{sl}(b \to D^{*+}\ell^- X)/P_{sl}(b \to D^0\ell^- X) = 0.33 \pm 0.09 \pm 0.05$.

In the systematic error, the contributions from the lepton identification and D^0 reconstruction cancel. This ratio is compatible with the value 0.50±0.15 observed at the $\Upsilon(4S)$ resonance [2] [9].

(ii) $f_d = 0.53 \pm 0.08$ ($stat$.DELPHI)±0.07 ($stat.\Upsilon(4S)$)± 0.10 ($syst.$) using the D^0 sample,

(iii) $f_d = 0.36 \pm 0.07$ ($stat$.DELPHI)± 0.09 ($stat.\Upsilon(4S)$)±0.07 ($syst.$) using the $D^{*+} \to (K^-\pi^+)\pi^+$ sample.

The systematic uncertainties come from the b semileptonic branching fraction, the lepton identification and the D reconstruction efficiencies. The VD efficiency was measured from the data by looking at the fraction of reconstructed D^0 where the two particles ($K\pi$) have associated hits in the VD, in an inclusive D^{*+} sample where no VD information was required. A correction factor 0.97± 0.03 to the D^0 reconstruction efficiency of the Monte Carlo simulation was determined.

Some $c\bar{c}$ and $b\bar{b}$ events could produce a D meson associated to a 'fake' lepton, or a 'fake' D meson associated to a lepton. These events were neglected because no $D^+\ell^+$ or $D^{*+}\ell^+$ pair was found in the data sample. Similarly the number of D^0 candidates has been found negligible in the wrong sign $K^+\pi^-\ell^-$ sample : as the wrong assignment of the kaon mass among the two particles of a true D^0 may mimic a wider D^0 peak, this contribution was estimated from simulation and subtracted before evaluating the amount of $K^+\pi^-\ell^-$ candidates.

It is important to notice that the above method does not depend of the exact source (B^- or $\bar{B}^0$) of the D^0 or D^{*+} mesons since it is based on the total D production from these two $\bar{B}$ mesons.

The combined result gives, taking into account the sources of systematics common to both analyses : $f_d = 0.45 \pm 0.08(stat.)\pm 0.09(syst.)$. This value of f_d is slightly overestimated since all the observed D^0 or D^{*+} were assumed to come only from B^- and $\bar{B}^0$ mesons. Since the probability of b quarks producing $\bar{B}_s$ and Λ_b is 1-2f_d , and assuming that the fraction of their semileptonic decays to D^0 or D^{*+} is 0.10±0.10, f_d is reduced by 0.01 :

$$f_d = 0.44 \pm 0.08(stat.) \pm 0.09(syst.)$$

This is the first direct measurement of this parameter which is relevant to the determination of the mixing properties of B^0 and B_s mesons, and where a value of $2f_d$ =0.75 is usually assumed.

In order to check that most $D^{*+}\ell^-$ originate from a $\bar{B}^0$ decay, the total measured $D^{*+}\ell^-$ production can be compared with the expectation for the exclusive decay $\bar{B}^0 \to D^{*+}\ell^-\bar{\nu}$. At LEP this is given by the $b \to \bar{B}^0$ production fraction, f_d , times the ratio of the branching fractions $Br(\bar{B}^0 \to D^{*+}\ell^-\bar{\nu})/Br(\bar{B}^0 \to X\ell^-\bar{\nu})$. These branching fractions are $4.8 \pm 0.4 \pm 0.4\%$ [3] [12] [14] and $9.9 \pm 3.0 \pm 0.9\%$ [15], respectively. Hence the expected fraction for the exclusive process is 0.21±0.09 to be compared with the observed value of 0.28±0.08 for all $D^{*+}\ell^-$ production, part of the errors being correlated. The $D^{*+}\ell^-$ sample is thus dominated by the $\bar{B}^0$ decay channel but there is room for some contribution from B^- through D^{**} contribution (see section 7).

Finally, assuming that the b quark always produces $\bar{B}^0$, B^- , $\bar{B}_s$ or Λ_b, the sum of $\bar{B}_s$ and Λ_b production can be derived, although with a large uncertainty :

$$f_{\bar{B}_s} + f_{\Lambda_b} = 1 - 2f_d = 0.12 \pm 0.16(stat.) \pm 0.18(syst.)$$

5 B energy reconstruction

The estimate of the B energy was based on the 'residual' energy taken by the hadronization particles accompanying the B meson. It was assumed that the only non-reconstructed particle in the lepton hemisphere (where the hemisphere axis is the thrust axis) is the neutrino of the B semileptonic decay. Then the residual energy is the total energy reconstructed in the lepton hemisphere less the energy already associated to the B decay products (lepton and D meson). The B energy was estimated by subtracting this hadronization part from the beam energy. Since the residual energy represents only around 13 GeV, the estimated error will be of the order of 2 GeV and will lead to an error of 8% on the B energy. This method is thus quite powerful in principle but two systematic effects must be taken into account :

(i) When the B decays into a D^* or a D^{**}, the pions or photons coming from the excited D meson decay will be included in the residual energy computation, which leads to an underestimation of the B energy. To account for this, the D^0 energy has to be scaled according to the Monte Carlo simulation [7] by a factor 1.08 which includes the different D meson production fractions and the corresponding part of the energy taken by the final D^0 . The final result is a correction factor of 1.04 ± 0.02 on the B energy.

(ii) The residual energy may be only partially reconstructed, and it will therefore be underestimated. The induced overestimation of the B energy can be obtained from simulation and the correction factor is found to be 0.96 ± 0.01. As a check, the observed overall shape of the residual energy distribution is well reproduced by the Monte Carlo simulation.

This correction factor has also been determined using only the data in the following way. The B energy can also be analytically obtained from the equations of energy-momentum conservation, provided one has an estimator of the B flight direction, for which the thrust of the lepton's jet was used. In most of the cases two possible solutions are found and an algorithm has been defined to extract the best estimator of the B energy. The choice between the two possible solutions requires a rough a priori knowledge of the fragmentation function. Therefore, the algorithm cannot be used for the measurement of the b fragmentation function. But for a given choice of the B energy, this algorithm method was found to be quite robust to other systematic effects, such as the effect (i) mentioned above, and does not depend at all on the residual energy reconstruction. The comparison between the two methods shows that the B energy estimated from the residual energy reconstruction has to be decreased by 3.5%, in good agreement with the previous correction factor 0.96 ± 0.01.

In conclusion, these two effects (i) and (ii) are of the same order, and tend to compensate each other. The energy resolution is 8%, according to the Monte Carlo simulation. The residual energy method is not applicable for 20% of the events, due to badly measured charged or neutral particles which would give an estimate of the B energy much below the energy of the D-lepton system.

Another way to estimate the B momentum is to consider its correlation with the observed $D\ell^-$ momentum of the Monte Carlo simulation [7] where the D^{**} contribution is taken into account :

$$p(B) = p(D\ell^-)/[0.41 + 0.013p(D\ell^-)] \tag{4}$$

The corresponding momentum resolution is 14% in average and follows :

$$\sigma(p)/p(B) = 0.36 - 0.0082 \cdot p(D\ell^-)\ (\mathrm{GeV/c}) \tag{5}$$

These formula were used when the residual energy method was not applicable and for the B lifetime measurement.

The fragmentation distribution obtained using the D^0 data, after background subtraction and acceptance correction, is shown in Figure 8. It is the first measurement of the b fragmentation function where the energy of each B meson is individually reconstructed and constitutes therefore the most direct measurement of this fragmentation function to date.

In order to determine the mean B meson energy, the measured $X_E(B)$ was empirically fitted using a Peterson function [‡] (solid line of Figure 8) for $X_E(B)$ larger than 0.25. The mean value of the fitted distribution is :

$$< X_E(B) >= 0.695 \pm 0.015(stat.) \pm 0.029(syst.)$$

in good agreement with estimates from inclusive lepton spectra [17].

6 Average B lifetime using $D^0\ell^-$,$D^+\ell^-$ and $D^{*+}\ell^-$ samples

As already discussed in section 4, the $D^0\ell^-$ and $D^+\ell^-$ (or $D^{*+}\ell^-$) samples are dominated by B^- and $\bar{B}^0$ decays, respectively. In this section the B lifetime is measured in these $D\ell^-$ samples separately. In the next section the B^+ and B^0 lifetimes will be evaluated.

The B meson mean lifetime was determined from maximum likelihood fits to the B proper time distributions of the $D^0\ell^-$, $D^+\ell^-$ and $D^{*+}\ell^-$ samples. These used an analysis of the decay lengths shown diagrammatically in Figure 9. It is also possible to obtain the lifetime ratio of B^0 and B^+ by trying to extract their respective semileptonic branching fractions from the observed yields of the $D^0\ell^-$ and $D^+\ell^-$ (or $D^{*+}\ell^-$) samples. This is not done in the present analysis since it was found that the sensitivity of this method is smaller than the direct measurement of the lifetimes described below.

In order to enhance the secondary vertex resolution as well as to reject spurious vertices, the lepton was required to have hits associated in the Vertex Detector, with the same criteria as the $K\pi$ pair of the D^0 (see section 3.1). For $D^0\ell^-$ events, the maximum distance between the extrapolated tracks ($K\pi$) with respect to their common vertex in space was required to be less than 4 mm. Furthermore those D^0 already observed to be D^{*+} decay products were rejected. From the 92 initial $D^0\ell^-$ events, 78 candidates remained. Of these, 70 events gave a satisfactory D^0-lepton vertex and were used for the lifetime measurement.

The D^0 or D^+ momentum was computed with its error matrix at the measured $K\pi$, $K2\pi$ or $K3\pi$ secondary vertex in space. A D^0-lepton , D^+-lepton or D^0-lepton-π (in case of D^{*+}) vertex was then fitted in space. As the precision of the fitted vertex position is much better in the Rϕ plane, the coordinates of the secondary vertex were taken in this transverse plane. Considering the polar angle of the $D\ell^-$ total momentum system as a reliable estimate of the B direction, the B decay length was then computed in space. The B decay length was signed according to the $D\ell^-$ direction. The B meson momentum was obtained from the $D\ell^-$ measured momentum, using the formula given in section 5 (equ. 4). This formula was used for all events. The method of the residual

[‡] The Peterson fragmentation function [16] $D_Q(z) \propto 1/\left(z \cdot [1 - (1/z) - \varepsilon_b/(1-z)]^2\right)$ is defined with respect to $z = (E+P_l)_B/(E+P_l)_b$ and with the Peterson coefficient ε_b. Here it is used with respect to $X_E(B) = E_B/E_{beam}$ and with an effective coefficient ϵ.

energy, when applicable, was used for systematic cross-checks. The B proper time could thus be extracted on an event-by-event basis.

The proper time distribution of the combinatorial background below the D meson signals was evaluated by selecting some event samples in the neighbourhood of the D mass, as displayed in Table 1.

D meson signal	background sample	background $(K(\mathrm{n})\pi)$ mass range (MeV/c^2)	background ΔM range (MeV/c^2)
$D^0 \to K^-\pi^+$	$(K^-\pi^-)\ell^+$	1760–1960	—
	$(K^-\pi^+)\ell^+$	2000–2200	—
$D^+ \to K^-\pi^+\pi^+$	$(K^-\pi^+\pi^+)\ell^\pm$	1600–1800 or 1940–2140	>150
$D^{*+} \to (K^-\pi^+)\pi^+$	$(K^-\pi^+)\pi^+\ell^+$	1720–2000	<160
$D^{*+} \to (K^-\pi^+\pi^+\pi^-)\pi^+$	$(K^-\pi^+\pi^+\pi^-)\pi^+\ell^\pm$	1600–1700 or 2000–2100	150–155

Table 1: Selected background samples for the B lifetime determination.

If different K mass assignments were possible within the same set of $(K^-\pi^+\pi^+\pi^-)$ charged particles, then only one combination was retained for the proper time measurement and the signal-to-noise ratio was corrected.

The B meson mean lifetime τ was determined from the event-by-event maximum likelihood fit to the proper time distributions of the $D\ell^-$ samples. The input of the fit for each event was :

- the measured B decay length L with its measured error σ_L, computed from the error matrix of the primary and secondary vertices;
- the reconstructed B momentum p with its estimated error σ_p (equ. 5).

The resulting proper time $t_i = L/(\beta\gamma c) = (m_B/p)\cdot(L/c)$ with the uncertainty σ_i given by $(\sigma_i/t_i)^2 = (\sigma_L/L)^2 + (\sigma_p/p)^2$ were used to compute the probability $P(t_i, \sigma_i, \tau)$ of observing a proper time t_i within the interval $[t_1, t_2]$:

$$P(t_i, \sigma_i, \tau) = f(t_i, \sigma_i, \tau) \,/\, \int_{t_1}^{t_2} f(t, \sigma_i, \tau)\, dt \tag{6}$$

where $f(t_i, \sigma_i, \tau)$ is a convolution of an exponential $\exp(-t/\tau)$ with a Gaussian function of width σ_i :

$$f(t_i, \sigma_i, \tau) = \frac{1}{\tau\sigma_i\sqrt{2\pi}} \int_0^{+\infty} e^{-t/\tau} e^{-(t-t_i)^2/2\sigma_i^2} dt \tag{7}$$

$$= \frac{1}{2\tau} \cdot \exp\left[\frac{\sigma_i^2}{2\tau^2} - \frac{t_i}{\tau}\right] \cdot \mathrm{erfc}\left[\frac{1}{\sqrt{2}}\left(\frac{\sigma_i}{\tau} - \frac{t_i}{\sigma_i}\right)\right] \tag{8}$$

Two event samples were considered : the $D\ell^-$ sample itself with N_T events and an independent background sample with N_B' events. The mean lifetime τ was obtained from

the maximum of the log. likelihood function

$$\mathcal{L} = \frac{N_S}{N_T}\left[\sum_{i=1}^{N_T}\log P(t_i,\sigma_i,\tau) - r\sum_{i=1}^{N'_B}\log P(t_i,\sigma_i,\tau)\right] \tag{9}$$

with t_i as variable, and where $N_T = N_S + N_B$ is the sum of signal and noise events in the $D\ell^-$ sample and $r = N_B/N'_B$ is the statistical weight factor for the background sample. The factor N_S/N_T, which takes into account the background contribution (N_B) in the statistical error, allows different samples to be combined with their appropriate statistical weight. The fit was performed on all events with a proper time between -2 and $+10$ ps. For the samples where the D mesons were selected with a normalised decay length $\Delta L/\sigma$ greater than 1 or 1.5, the function $f(t_i,\sigma_i,\tau)$ was corrected using an acceptance function depending on t_i, derived from the Monte Carlo simulation. Without this acceptance correction, the fitted B lifetime would be overestimated by 5 % in average. The results are presented in Figure 10a-d and summarised in Table 2.

Figure	$\bar{B}$ decay	D decay	signal events	signal-to-noise ratio	B lifetime (ps)
10a	$D^0\ell^-X$	$D^0 \to K\pi$	70±12	2.0	$1.27^{+0.22}_{-0.18}(stat.)$
10b	$D^+\ell^-X$	$D^+ \to K\pi\pi$	30±7	1.6	$1.18^{+0.39}_{-0.27}(stat.)$
10c	$D^{*+}\ell^-X$	$D^{*+} \to (K\pi)\pi$	22±5	4.9	$1.03^{+0.34}_{-0.24}(stat.)$
10d	$D^{*+}\ell^-X$	$D^{*+} \to (K3\pi)\pi$	26±7	1.4	$1.33^{+0.41}_{-0.28}(stat.)$
	$D^{*+}\ell^-X$	$(K\pi)\pi$ and $(K3\pi)\pi$ combined fit			$1.19^{+0.25}_{-0.19}(stat.)$
	$D^{(*)+}\ell^-X$	D^+ and D^{*+} combined fit			$1.19^{+0.20}_{-0.16}(stat.)$
11	$D\ell^-X$	D^0, D^+ and D^{*+} combined fit			$1.23^{+0.14}_{-0.13}(stat.)$

Table 2: B lifetime measurements for the selected $\bar{B} \to D\ell^-X$ decays.

As a cross-check of the lifetime measurement method and of the analysis procedure, the decay length between the measured D^0-lepton or D^0-lepton-π vertex and the measured $K\pi$ vertex (Fig. 9) was used to fit the D^0 lifetime (Fig. 10e). Similarly the decay length between the measured D^+-lepton vertex and the measured $K\pi\pi$ vertex was used to fit the D^+ lifetime (Fig. 10f). The values found are:

$$\tau(D^0) = 0.439^{+0.073}_{-0.061}(stat.)\text{ ps} \quad\text{and}\quad \tau(D^+) = 0.87^{+0.30}_{-0.22}(stat.)\text{ ps}$$

They agree with the world average values 0.420±0.008 ps and 1.066±0.023 ps, respectively [8].

In summary, the B lifetime has been measured in $D^0\ell^-$, $D^+\ell^-$ and $D^{*+}\ell^-$ samples :

$$\begin{aligned}
\tau(B) &= 1.27^{+0.22}_{-0.18}(stat.) \pm 0.15(syst.)\text{ ps where } \bar{B} \to D^0\ell^-X \\
\tau(B) &= 1.18^{+0.39}_{-0.27}(stat.) \pm 0.15(syst.)\text{ ps where } \bar{B} \to D^+\ell^-X \\
\tau(B) &= 1.19^{+0.25}_{-0.19}(stat.) \pm 0.15(syst.)\text{ ps where } \bar{B} \to D^{*+}\ell^-X
\end{aligned}$$

where both $K\pi$ and $K3\pi$ modes of the $D^{*+}\ell^-$ sample were used in a combined fit. The different contributions to the systematic uncertainty are summarised in Table 3.

Systematic uncertainty	$\sigma_\tau/\tau(B)$ (%)
B momentum estimator (without D^{**} contribution)	6
D^{**} contribution to the B momentum	2
B decay length reconstruction method	9
Evaluation of the B decay length error σ_L	2
Acceptance ($\Delta L/\sigma$ selection)	3
Choice of the proper time interval	3
Signal-to-noise ratio	1
Total	12

Table 3: Contributions to the systematic uncertainty of the measured B lifetime.

Evaluating the B momentum from a formula (equ.4) or from the residual energy method, as explained in section 5, changes the measured B lifetime by 6 %. The systematic uncertainty of 9 % due to the reconstruction of the B decay length was estimated by computing the primary interaction vertex with different selections for the charged particles.

As already discussed in section 4, part of the $D^{*+}\ell^-$ sample is produced by the decay $B \to D^{*+}\bar{D}X$ followed with a semileptonic decay of the $\bar{D}$ daughter. As a p_T cut is applied on half of the D^{*+} (into $(K3\pi)\pi$) sample, this contamination affects only 7% of the $D^{*+}\ell^-$ events on which the change in the measured B lifetime was found small according to the simulation. This contribution was thus neglected.

The full sample can also be used to determine an averaged B meson lifetime using semileptonic events together with a reconstructed charmed D meson (Fig. 11) :

$$\tau(B) \;=\; 1.23^{+0.14}_{-0.13}(stat.) \pm 0.15(syst.)\ \text{ps}$$

Note that this result uses more information than results based on the impact parameter of the lepton only [17].

7 B^+ and B^0 lifetimes

Inside the $D^{(*)}\ell^-$ samples [§] , the relative proportions of B^+ and B^0 mesons have to be evaluated in order to determine the B^+ and B^0 lifetimes. As discussed earlier, decays to D^0 and $D^{(*)+}$ can occur through $B^- \to D^{(*)0}\ell^-\bar{\nu}$ or $\bar{B}^0 \to D^{(*)+}\ell^-\bar{\nu}$ decays, as well as by decays to a D^{**} excited state, or to nonresonant $D^{(*)}(\mathrm{n})\pi$.

Some D^{**} mesons have been observed at lower energies [18] [19] and in photoproduction [20]. These states have a mass of about 2.42 and 2.46 GeV/c^2 and their favored

[§] Hereafter the notation $D^{(*)}$ will stand for a D meson or as well for a D^* meson

spin-parities are : $J^P = 1^+$ for the lower and $J^P = 2^+$ for the higher D^{**} mass. According to the CLEO experiment at the $\Upsilon(4S)$, only 64±12% of B meson semileptonic decays occur through the channels $\bar{B} \to D\ell^-\bar{\nu}$ and $\bar{B} \to D^*\ell^-\bar{\nu}$ [2]. Thus 36±12% are due to D^{**} or nonresonant $D^{(*)}(n)\pi$ production (called also D^{**} for simplification in the following). If these D^{**} mesons decay into $D^{(*)}\pi$, they can contribute to the $D^0\ell^-$ and $D^{(*)+}\ell^-$ samples. In fact they have two consequences : the main one is that a D^{**} may decay into $D^*\pi$ or into $D\pi$, thus mixing the relative proportions of $\bar{B}^0$ and B^- in the $D\ell^-$ samples. In addition the reconstructed B momentum has to be corrected for the unseen soft pion(s) from the D^{**}, as already mentioned in section 5.

Another source of dilution is the non-reconstruction of the bachelor pion in the decay $\bar{B} \to D^{*+}\ell^- X$ followed by $D^{*+} \to D^0\pi^+$. Since 15±2% of the reconstructed D^0 are measured to come from a D^{*+} decay and since the reconstruction efficiency of the bachelor pion is 75±5%, only 8±3% of the remaining $D^0\ell^-$ events originate from a $\bar{B}^0$ due to this mechanism. This dilution is small compared to the D^{**} contribution, but is taken into account.

The relative amounts of B^- and $\bar{B}^0$ mesons inside the $D^0\ell^-$ and $D^{(*)+}\ell^-$ samples are detailed in the Appendix. When normalising the different contributions, the lifetimes $\tau(B^+)$ and $\tau(B^0)$ of the B^+ and B^0 mesons can be obtained by a combined fit on the three data samples ($D^0\ell^-$, $D^+\ell^-$ and $D^{*+}\ell^-$) where the probability $P(t_i, \sigma_i, \tau)$ involved in equation 9 is expressed as :

$$(1-\alpha)\cdot P(t_i,\sigma_i,\tau(B^+)) + \alpha \cdot P(t_i,\sigma_i,\tau(B^0)) \quad \text{for} \quad \bar{B} \to D^0\ell^- X \tag{10}$$

$$(1-\beta_+)\cdot P(t_i,\sigma_i,\tau(B^0)) + \beta_+ \cdot P(t_i,\sigma_i,\tau(B^+)) \quad \text{for} \quad \bar{B} \to D^+\ell^- X \tag{11}$$

$$(1-\beta_*)\cdot P(t_i,\sigma_i,\tau(B^0)) + \beta_* \cdot P(t_i,\sigma_i,\tau(B^+)) \quad \text{for} \quad \bar{B} \to D^{*+}\ell^- X \tag{12}$$

with $\alpha = 0.28^{+0.05}_{-0.05}$, $\beta_+ = 0.25^{+0.08}_{-0.10}$, $\beta_* = 0.20^{+0.09}_{-0.12}$ where the error reflects the uncertainty on the $\bar{B}$ branching fractions into $D\ell^- X$ final states.

The charged and neutral B meson lifetimes are found to be :

$$\begin{aligned}
\tau(B^+) &= 1.30^{+0.33}_{-0.29}(stat.) \pm 0.15(syst.exp.) \pm 0.05(syst.D^{**}) \text{ ps} \\
\tau(B^0) &= 1.17^{+0.29}_{-0.23}(stat.) \pm 0.15(syst.exp.) \pm 0.05(syst.D^{**}) \text{ ps} \\
\tau(B^+)/\tau(B^0) &= 1.11^{+0.51}_{-0.39}(stat.) \pm 0.05(syst.exp.) \pm 0.10(syst.D^{**})
\end{aligned}$$

where the systematic errors are subdivided into two contributions : first an experimental uncertainty detailed in Table 3, and second the uncertainty on the $\bar{B} \to D\ell^- X$ branching fractions.

8 Conclusion

This analysis of charmed D mesons associated with a lepton in the same direction has been performed with the DELPHI detector at LEP. From the 1991 data sample, 92 $D^0\ell^-$, 35 $D^+\ell^-$ and 61 $D^{*+}\ell^-$ have been isolated. From the $D^0\ell^- X$ and $D^{*+}\ell^- X$ yield, the probability that a b quark hadronizes as a $\bar{B}^0$ (or a B^-) meson is found to be f_d =0.44±0.08±0.09, corresponding to a total $(B_s + \Lambda_b)$ hadronization fraction of 0.12±0.24. This is the first direct measurement of the f_d parameter which is relevant to the determination of the mixing properties of B^0 and B_s mesons. In past analyses a value of $2f_d$ =0.75 has usually been assumed.

The fragmentation function of the b quark has been obtained for the first time by reconstructing the energy of each individual B meson. It is in agreement with previous

inclusive measurements. The mean value of the B meson energy, expressed in terms of the beam energy, is :

$$< X_E(B) >= 0.695 \pm 0.015(stat.) \pm 0.029(syst.)$$

The following mean B lifetimes have been directly measured :

$$\begin{aligned}
\tau(B) &= 1.27^{+0.22}_{-0.18}(stat.) \pm 0.15(syst.) \text{ ps where } \bar{B} \to D^0 \ell^- X \\
\tau(B) &= 1.18^{+0.39}_{-0.27}(stat.) \pm 0.15(syst.) \text{ ps where } \bar{B} \to D^+ \ell^- X \\
\tau(B) &= 1.19^{+0.25}_{-0.19}(stat.) \pm 0.15(syst.) \text{ ps where } \bar{B} \to D^{*+} \ell^- X
\end{aligned}$$

and $\tau(B) = 1.23^{+0.14}_{-0.13}(stat.) \pm 0.15(syst.)$ ps from all three data samples. These are in good agreement with the averaged semileptonic B lifetime measured at LEP ($\tau(B) = 1.33 \pm 0.05 \pm 0.06$ ps [17]).

The contribution from the decays $\bar{B} \to D^{**} \ell^- \bar{\nu}$ is estimated from measurements at the $\Upsilon(4S)$ energy, where D^{**} stands for an excited charmed meson or for nonresonant $D^{(*)}(\mathrm{n})\pi$ final states. Assuming that this contribution is the same for B^0 or B^+ semileptonic decays, and with reasonable assumptions on the D^{**} branching fractions, then the lifetimes of charged and neutral B mesons are :

$$\begin{aligned}
\tau(B^+) &= 1.30^{+0.33}_{-0.29}(stat.) \pm 0.15(syst.exp.) \pm 0.05(syst.D^{**}) \text{ ps} \\
\tau(B^0) &= 1.17^{+0.29}_{-0.23}(stat.) \pm 0.15(syst.exp.) \pm 0.05(syst.D^{**}) \text{ ps} \\
\tau(B^+)/\tau(B^0) &= 1.11^{+0.51}_{-0.39}(stat.) \pm 0.05(syst.exp.) \pm 0.10(syst.D^{**})
\end{aligned}$$

The B^+ and B^0 lifetimes are found equal within errors. This result is compatible with indirect measurements of $\tau(B^+)/\tau(B^0)$ at the $\Upsilon(4S)$ energy [2] [3]. It suggests, as opposed to the charm case where D^+ and D^0 lifetimes differ by a factor 2.5, that the spectator model [1] is a good tool for the understanding of B decays.

Acknowledgements

We are greatly indebted to our technical collaborators and to the funding agencies for their support in building and operating the DELPHI detector, and to the members of the CERN-SL Division for the excellent performance of the LEP collider.

Appendix

In this Appendix the various inputs necessary to extract the B^+ and B^0 lifetimes are summarised. The following B branching fractions have been computed from the average of the last CLEO [2] [14] and ARGUS [3] results [12] :

- $Br(B^- \to D^0\ell^-\bar{\nu}) + Br(B^- \to D^{*0}\ell^-\bar{\nu}) = 6.7 \pm 0.8 \pm 1.0\%$ (denoted b_0)
- $Br(\bar{B}^0 \to D^+\ell^-\bar{\nu}) = 1.9 \pm 0.5 \pm 0.2\%$ (denoted b_+)
- $Br(\bar{B}^0 \to D^{*+}\ell^-\bar{\nu}) = 4.8 \pm 0.4 \pm 0.4\%$ (denoted b_*)
- $Br(\bar{B} \to D^{**}\ell^-\bar{\nu}) = Br(\bar{B} \to X\ell^-\bar{\nu}) - Br(\bar{B} \to D^{(*)}\ell^-\bar{\nu}) = 3.8 \pm 1.0\%$ where $Br(\bar{B} \to X\ell^-\bar{\nu}) = 10.5 \pm 0.5\%$ [8]. According to the Monte Carlo simulation, the selection efficiencies for $D^{**}\ell^-$ and $D^{(*)}\ell^-$ events differ by a factor 0.90 ± 0.05. As only a relative selection efficiency is involved for the B lifetime measurement, an effective branching fraction b_{**} is used :

$$b_{**} = Br(\bar{B} \to D^{**}\ell^-\bar{\nu}) \cdot (0.90 \pm 0.05) = 3.4 \pm 0.9\%$$

Only an averaged D^{**} production rate can be deduced from the above references. It will be further assumed that :

- $Br(\bar{B}^0 \to D^{**+}\ell^-\bar{\nu}) = Br(B^- \to D^{**0}\ell^-\bar{\nu}) = b_{**}$
- $Br(D^{**+} \to D^{(*)0}\pi^+) = 2 \cdot Br(D^{**+} \to D^{(*)+}\pi^0)$ and
  $Br(D^{**0} \to D^{*+}\pi^-) = 2 \cdot Br(D^{**0} \to D^{*0}\pi^0)$ (due to isospin rules)
- $Br(D^{**} \to D\pi)/Br(D^{**} \to (D \text{ or } D^*)\pi) = \varepsilon \simeq 0.$ or 0.6–0.8 in case of 1^+ or 2^+ spin-parity states [10] [21] (a value $\varepsilon = 0.4 \pm 0.4$ was used).
- Finally as already mentioned, the probabilities for a b quark to fragment into a $\bar{B}^0$ or into a B^- are considered equal.

The content of the $D\ell^-$ samples can then be classified as shown in Table 4.

	$\bar{B}$ decay	$D^0\ell^-$	$D^+\ell^-$	$D^{*+}\ell^-$
a_1	$B^- \to D^{(*)0}\ell^-\bar{\nu}$	b_0		
a_2	$\bar{B}^0 \to D^+\ell^-\bar{\nu}$		b_+	
a_3	$\bar{B}^0 \to D^{*+}\ell^-\bar{\nu}$	$b_*\eta\varepsilon_\pi$	$b_*(1-\eta)$	b_*
a_4	$B^- \to D^{**0}\ell^-\bar{\nu}$ with $D^{**0} \to D^{(*)0}\pi^0$ or $D^{(*)+}\pi^-$	$\frac{1}{3}b_{**}$ $+\frac{2}{3}b_{**}(1-\varepsilon)\eta\varepsilon_\pi$	$\frac{2}{3}b_{**}\varepsilon$ $+\frac{2}{3}b_{**}(1-\varepsilon)(1-\eta)$	$\frac{2}{3}b_{**}(1-\varepsilon)$
a_5	$\bar{B}^0 \to D^{**+}\ell^-\bar{\nu}$ with $D^{**+} \to D^{(*)0}\pi^+$ or $D^{(*)+}\pi^0$	$\frac{2}{3}b_{**}$ $+\frac{1}{3}b_{**}(1-\varepsilon)\eta\varepsilon_\pi$	$\frac{1}{3}b_{**}\varepsilon$ $+\frac{1}{3}b_{**}(1-\varepsilon)(1-\eta)$	$\frac{1}{3}b_{**}(1-\varepsilon)$

Table 4: Branching fractions of $\bar{B}$ decays contributing to each $D\ell^-$ sample ($\eta = Br(D^{*+} \to D^0\pi^+) = 0.68 \pm 0.03$ as measured by the CLEO II collaboration [12], $1 - \varepsilon_\pi = 0.75 \pm 0.05$ is the reconstruction efficiency of the bachelor pion in the decay $D^{*+} \to D^0\pi^+$).

The semileptonic decays of B_s and Λ_b are neglected : only $10 \pm 10\%$ of these semileptonic decays are expected to produce D^0 or $D^{(*)+}$ mesons, their contribution is negligible

if the B_s and Λ_b lifetimes are close to the B^+ and B^0 lifetimes. The α, β_+ and β_* parameters of section 7 (equ. 10-12) are computed as :

$$\alpha = \left[a_3(D^0\ell^-) + a_5(D^0\ell^-)\right] / \left[\sum_{i=1}^{5} a_i(D^0\ell^-)\right] \quad (13)$$

$$\beta_+ = a_4(D^+\ell^-) / \left[\sum_{i=2}^{5} a_i(D^+\ell^-)\right] \quad (14)$$

$$\beta_* = a_4(D^{*+}\ell^-) / \left[\sum_{i=3}^{5} a_i(D^{*+}\ell^-)\right] \quad (15)$$

The results are : $\alpha = 0.28^{+0.05}_{-0.05}$, $\beta_+ = 0.25^{+0.08}_{-0.10}$, $\beta_* = 0.20^{+0.09}_{-0.12}$ where the error reflects the uncertainty on the $\bar{B}$ branching fractions into $D\ell^-X$ final states.

References

[1] H. Fritzsch and P. Minkowski: Phys. Rep. **73** (1981) 67.

[2] CLEO coll., R. Fulton et al.: Phys. Rev. **D43** (1991) 651.

[3] ARGUS coll., H. Albrecht et al.: Preprint DESY 92-029 (1992).

[4] DELPHI coll., P. Aarnio et al.: Nucl. Inst. and Meth. **A303** (1991) 233.

[5] DELPHI coll., E. Anassontzis et al., 'The Barrel RICH of DELPHI', to appear in : Proc. 1992 Wire Chamber Conference (Vienna, Austria, 1992).

[6] DELPHI coll., P. Abreu et al.: Preprint CERN-PPE/92-79, to be published in Z. Phys. C.

[7] T. Sjostrand: Comp. Phys. Comm. **39** (1986) 347;
T. Sjostrand and M. Bengtsson: Comp. Phys. Comm. **43** (1987) 367;
T. Sjostrand: JETSET 7.3 manual, preprint CERN-TH.6488/92 (1992).

[8] Review of Particle Properties (Particle Data Group): Phys. Rev. **D45** (1992).

[9] N. Katayama (CLEO coll.): Proceedings of the Heavy Quark Physics Symposium, Ithaca (1989), eds. P. Drell and D. Rubin, AIP conference proceedings.

[10] S. Godfrey and N. Isgur: Phys. Rev. **D32** (1985) 189.

[11] CLEO coll., D. Bortoletto et al.: Phys. Rev. **D45** (1992) 21;
ARGUS coll., H. Albrecht et al.: Z. Phys. **C48** (1990) 583.

[12] The $\Upsilon(4S)$ and DELPHI results are presented taking the world average value for the D^0 and D^+ decays [8] and the new value 0.68 ± 0.03 for the $D^{*+} \to D^0\pi^+$ branching fraction (see for instance : D. Akerib (CLEO II coll.), XXVIIth Rencontres de Moriond (1992), Electroweak Interactions and Unified Theories).

[13] L3 coll., B. Adeva et al.: Phys. Lett. **B241** (1990) 416; Phys. Lett. **B261** (1991) 177;
ALEPH coll., D. Decamp et al.: Phys. Lett. **B244** (1990) 551;
OPAL coll., M.Z. Akrawy et al.: Phys. Lett. **B263** (1991) 311; P.D. Acton et al.: Z. Phys. **C55** (1992) 191.

[14] CLEO coll., D. Bortoletto et al.: Phys. Rev. Lett. **63** (1989) 1667.

[15] CLEO coll., S. Henderson et al.: Phys. Rev. **D45** (1992) 2212.

[16] C.Peterson et al., Phys. Rev. **D27** (1983) 105.

[17] P. Roudeau, Heavy flavour physics at LEP, in : Proc. Joint International Symposium & Europhysics Conference on High Energy Physics (Geneva, Switzerland, 25 July-1 August 1991), Vol.2, eds. S. Hegarty, K. Potter, E. Quercigh (World Scientific, Singapore, 1992) p.301.

[18] ARGUS coll., H. Albrecht et al.: Phys. Rev. Lett. **56** (1986) 549; ARGUS coll., H. Albrecht et al.: Phys. Lett. **B221** (1989) 422; ARGUS coll., H. Albrecht et al.: Phys. Lett. **B232** (1989) 398.

[19] CLEO coll., P. Avery et al.: Phys. Rev. **D41** (1990) 774.

[20] E691 coll., J.C. Anjos et al.: Phys. Rev. Lett. **62** (1989) 1717.

[21] L. Rosner: Comments Nucl. Part. Phys. **16** (1986) 109.

Figure Captions

Figure 1: Distributions of the difference between the observed dE/dx and the expected kaon ionization loss :

(a) for a kaon enriched sample (unhatched histogram) and a pion enriched sample (hatched histogram). These two samples have been selected using the RICH Cherenkov counter for charged particles between 8 and 15 GeV/c.

(b) for the particles having the same charge as the lepton in the $D^0 \to K^-\pi^+$ signal (kaon candidates).

Figure 2: (a) Distribution of the distance in the Rϕ plane between the secondary vertex formed by a pair of charged particles with an invariant mass above 1.5 GeV/c^2 and the primary vertex. (b) Distribution for the same quantity divided by its error.

Figure 3: $K^-\pi^+$ mass distribution from semileptonic events. The points corresponds to the K mass assignment for the particle in same direction ($\vec{p}(\ell^-) \cdot \vec{p}(K^-) > 0$) and with the same charge as the lepton. The lepton transverse momentum is above 1 GeV/c and the apparent decay length of the $K\pi$ pair fulfills $\Delta L/\sigma > 1$. The curve is a fit with three contributions : an exponential background (dashed line), a parametrisation of the $D^0 \to K^-\pi^+(\pi^0)$ signal where the π^0 is not detected ($K^-\pi^+$ mass below 1.8 GeV/c^2), and a Gaussian shape for the $D^0 \to K^-\pi^+$ signal.

Figure 4: Background subtracted and acceptance corrected $X_E(D)$ distribution of the reconstructed D^0 events (points). The histogram corresponds to the Monte Carlo simulation $\bar{B} \to D^0\ell^-X$ [7].

Figure 5: Apparent proper time distribution of the reconstructed D^0 mesons after background subtraction. The solid line (arbitrary normalisation) corresponds to the expected behaviour of D mesons directly produced by charm quarks and the histogram to D mesons originating from B decays.

Figure 6: $K^-\pi^+\pi^+$ mass distribution obtained on semileptonic events where the kaon candidate and the associated lepton of same direction have the same charge (solid line histogram : $\vec{p}(\ell^-)\cdot\vec{p}(K^-) > 0$) or opposite charge (hatched histogram :$\vec{p}(\ell^+)\cdot\vec{p}(K^-) > 0$). The selections are described in the text (see section 3.2). The curve is a fit where the background is described by a linear function and the signal by a Gaussian.

Figure 7: ΔM=M($(K^-\pi^+)\pi^+$)-M($K^-\pi^+$) (a), and ΔM=M($(K^-\pi^+\pi^+\pi^-)\pi^+$)-M($K^-\pi^+\pi^+\pi^-$) (b) distributions for events where the kaon candidate and the associated lepton of same direction have the same charge (solid line histogram :$\vec{p}(\ell^-) \cdot \vec{p}(K^-) > 0$) or opposite charge (hatched histogram :$\vec{p}(\ell^+) \cdot \vec{p}(K^-) > 0$). The ($K\pi$) or ($K3\pi$) mass interval is 1820<M<1900 MeV/c^2 and the selections are described in the text (see section 3.3). The curve is a fit to the sum of a Gaussian and of a function $\alpha(\Delta\text{M-}m_\pi)^\beta$ in order to describe the signal and the background, respectively.

Figure 8: Distribution of $X_E(B)$, the B meson energy divided by the beam energy. The points represent the data, after background subtraction and acceptance correction. The solid line is a fit to the data with a Peterson function (see footnote of section 5) when $X_E(B) > 0.25$.

Figure 9: Sketch of a $\bar{B}^0 \to D^{*+}\ell^-\bar{\nu}$ event followed by $D^{*+} \to D^0\pi^+$ and $D^0 \to K^-\pi^+$: primary interaction vertex (V_P), B decay vertex (V_B) and D^0 decay vertex (V_D).

Figure 10: Measured B proper time distributions in the four data samples after background subtraction : $\bar{B} \to D^0\ell^-X$ followed by $D^0 \to K^-\pi^+$ (a) , $\bar{B} \to D^+\ell^-X$ followed by $D^+ \to K^-\pi^+\pi^+$ (b) , $\bar{B} \to D^{*+}\ell^-X$ followed by $D^{*+} \to (K^-\pi^+)\pi^+$ (c) or $D^{*+} \to (K^-\pi^+\pi^+\pi^-)\pi^+$ (d) ; and measured D^0 and D^+ proper time distributions with D^0 decaying into $K^-\pi^+$ (e) and D^+ decaying into $K^-\pi^+\pi^+$ (f), respectively. The curves are the result of an event-by-event maximum likelihood fit where the normalised background distribution was subtracted. The fitting interval is $[-2.0, +10.0]$ ps.

Figure 11: Measured B proper time distribution when adding the four data samples after background subtraction : $\bar{B} \to D^0\ell^-X$ followed by $D^0 \to K^-\pi^+$, $\bar{B} \to D^+\ell^-X$ followed by $D^+ \to K^-\pi^+\pi^+$, $\bar{B} \to D^{*+}\ell^-X$ followed by $D^{*+} \to (K^-\pi^+)\pi^+$ or $D^{*+} \to (K^-\pi^+\pi^+\pi^-)\pi^+$. The curve is the result of an event-by-event maximum likelihood fit where the normalised background distribution was subtracted. The fitting interval is $[-2.0, +10.0]$ ps.

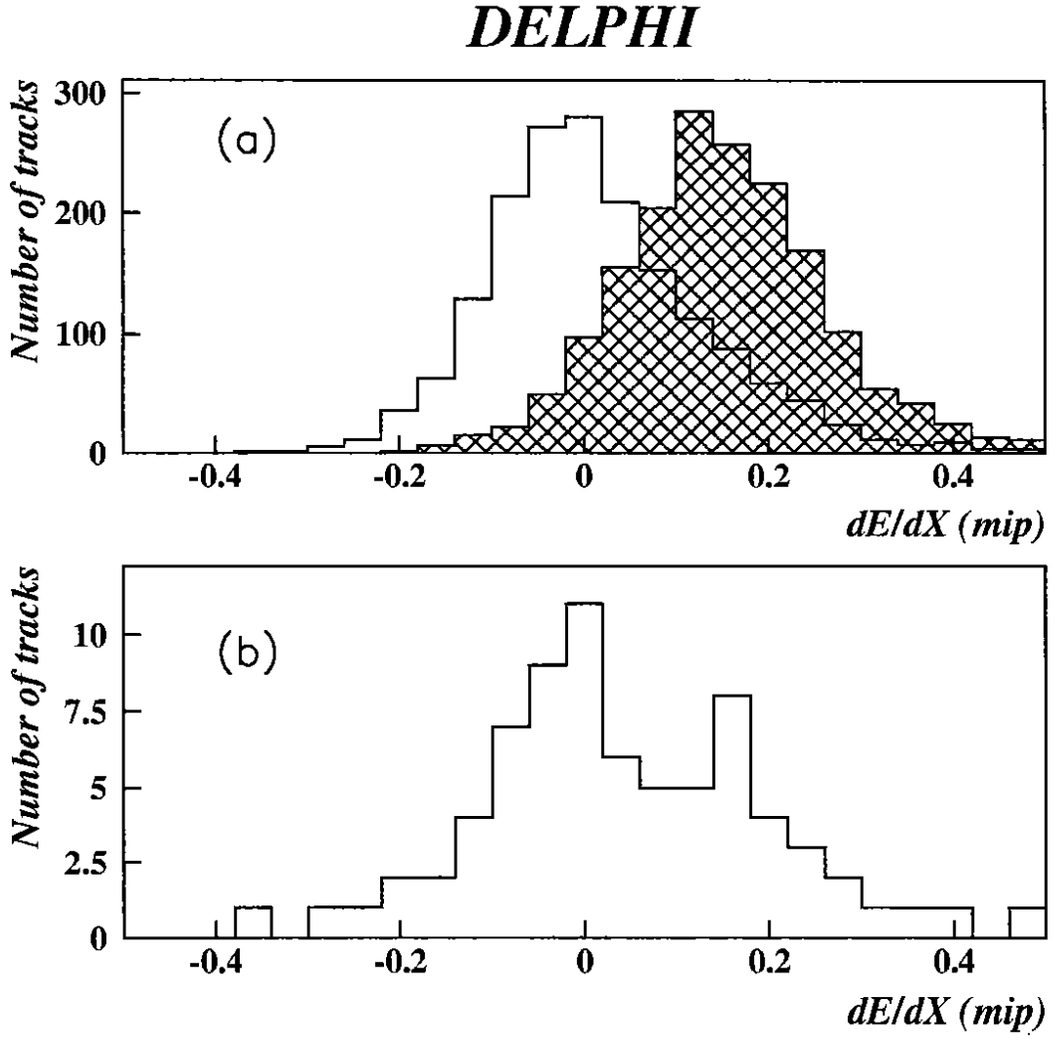
DELPHI
(a)
Number of tracks
300
200
100
0
-0.4
-0.2
0
0.2
0.4
dE/dX (mip)
(b)
Number of tracks
10
7.5
5
2.5
0
-0.4
-0.2
0
0.2
0.4
dE/dX (mip)

Figure 1:

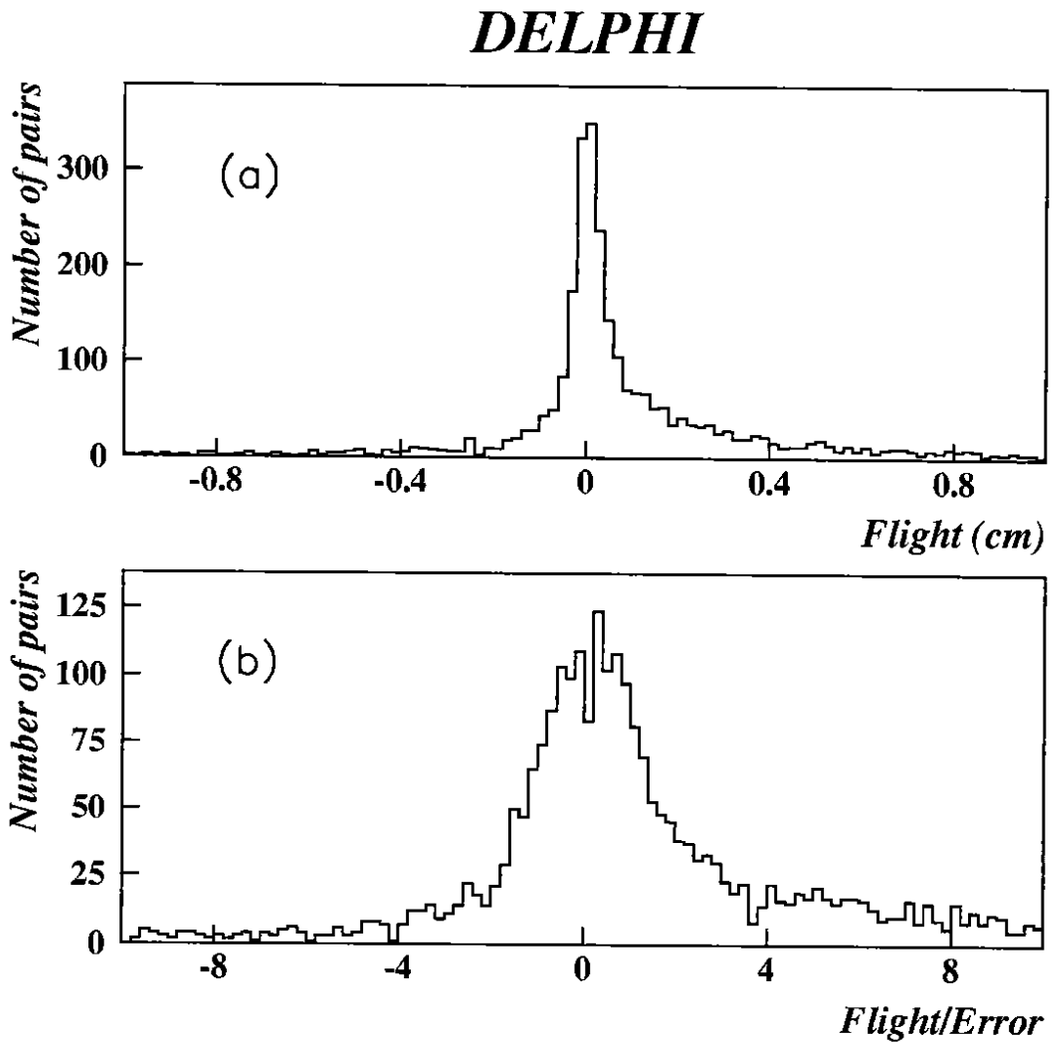
DELPHI
(a)
Number of pairs
300
200
100
0
-0.8
-0.4
0
0.4
0.8
Flight (cm)
(b)
Number of pairs
125
100
75
50
25
0
-8
-4
0
4
8
Flight/Error

Figure 2:

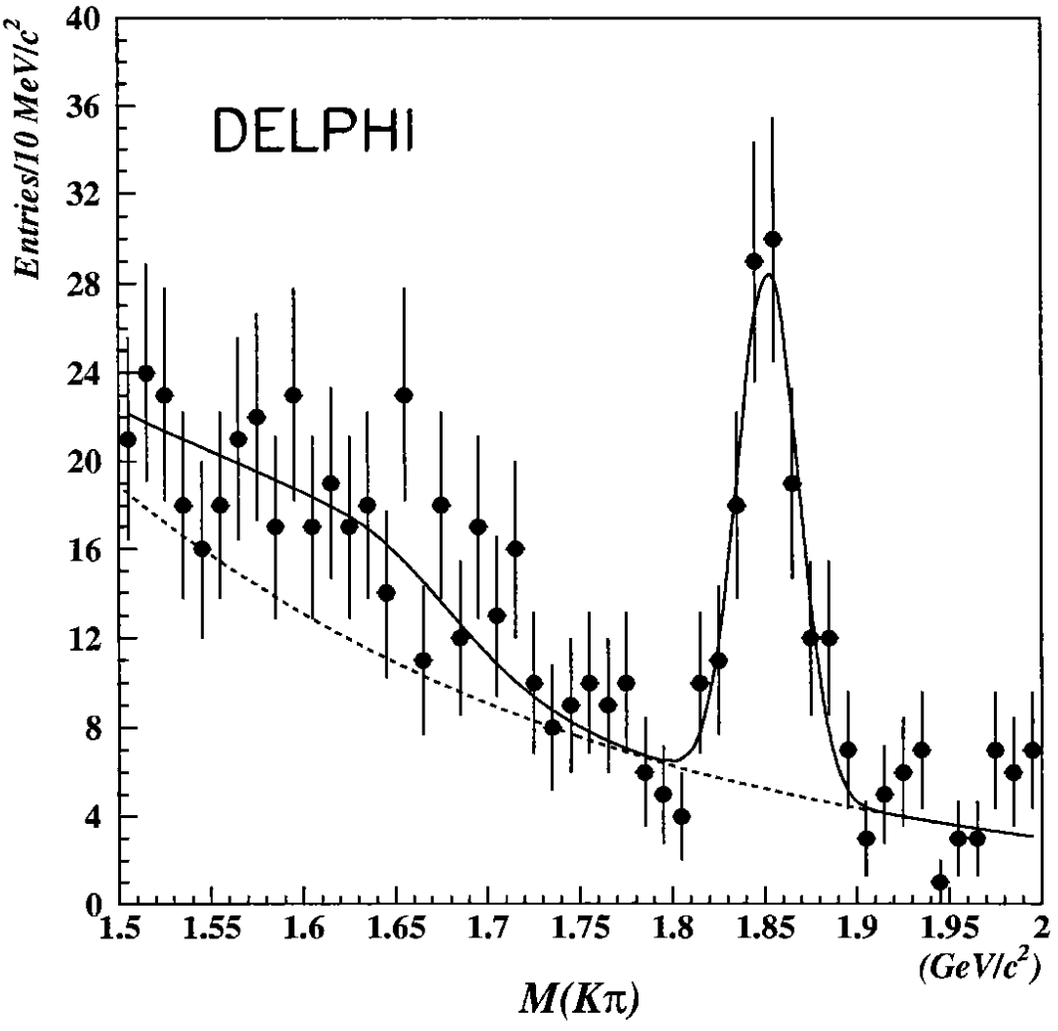
DELPHI
Entries/10 MeV/c²
40
36
32
28
24
20
16
12
8
4
0
1.5
1.55
1.6
1.65
1.7
1.75
1.8
1.85
1.9
1.95
2
(GeV/c²)
M(Kπ)

Figure 3:

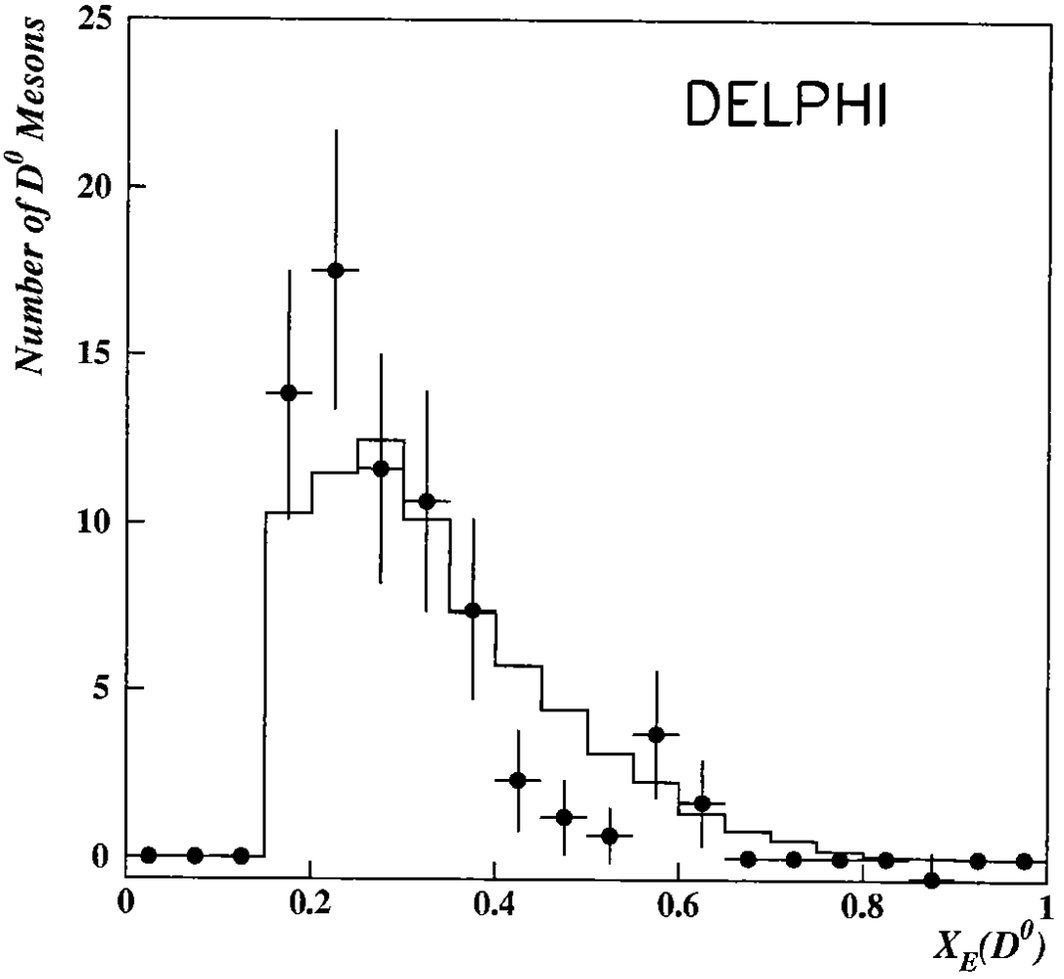

Figure 4:

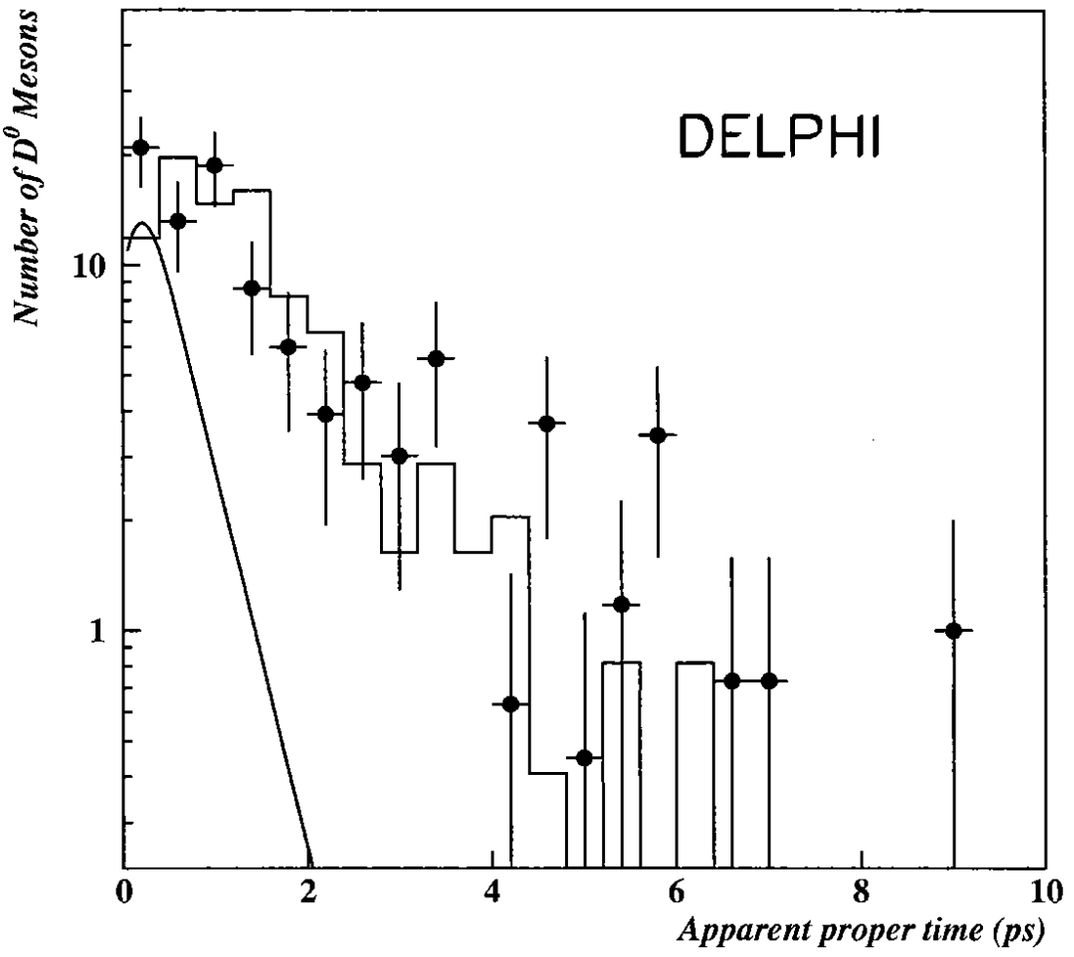
DELPHI
Number of D^0 Mesons
10
1
0
2
4
6
8
10
Apparent proper time (ps)

Figure 5:

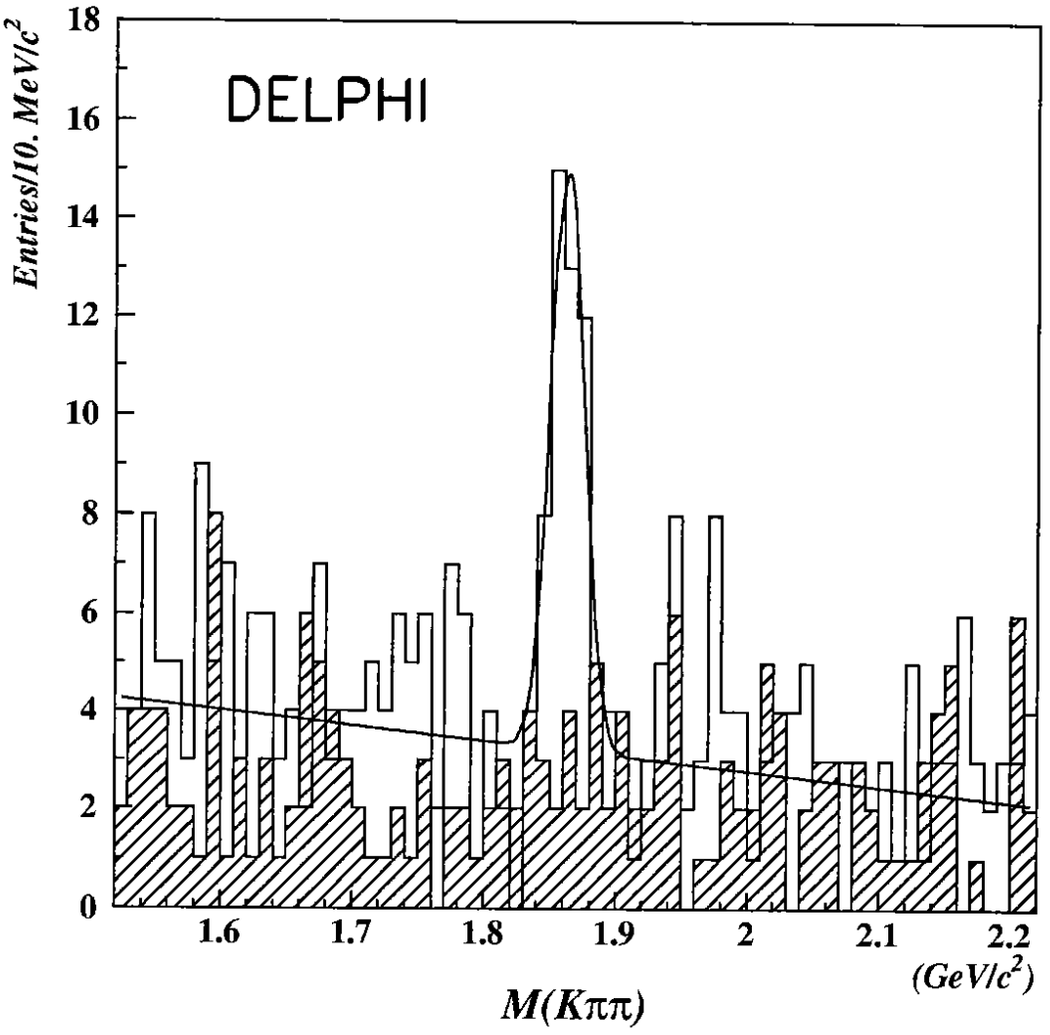
DELPHI
Entries/10. MeV/c²
18
16
14
12
10
8
6
4
2
0
1.6
1.7
1.8
1.9
2
2.1
2.2
(GeV/c²)
M(Kππ)

Figure 6:

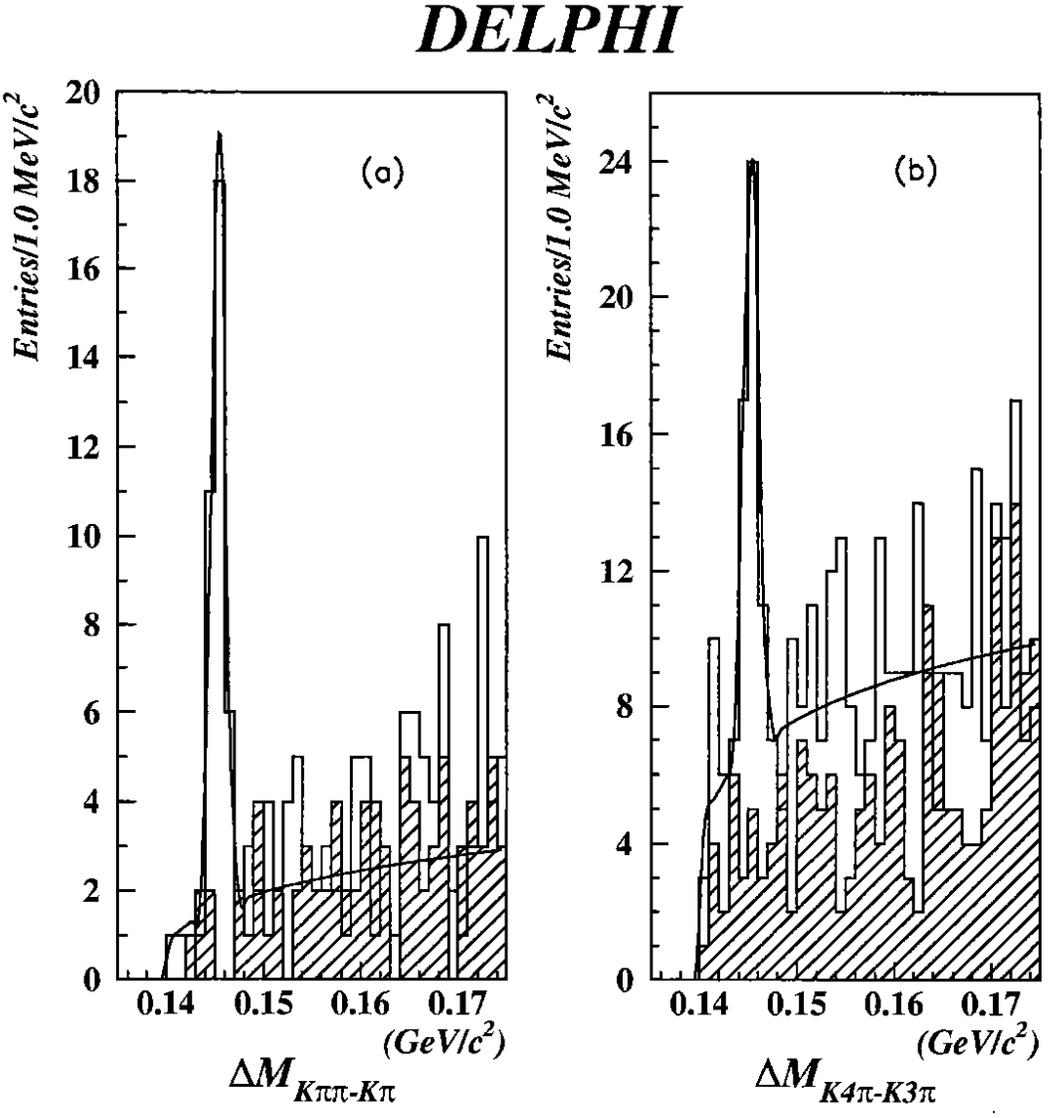
DELPHI
Entries/1.0 MeV/c²
(a)
(b)
0.14
0.15
0.16
0.17
(GeV/c²)
ΔM Kππ-Kπ
ΔM K4π-K3π

Figure 7:

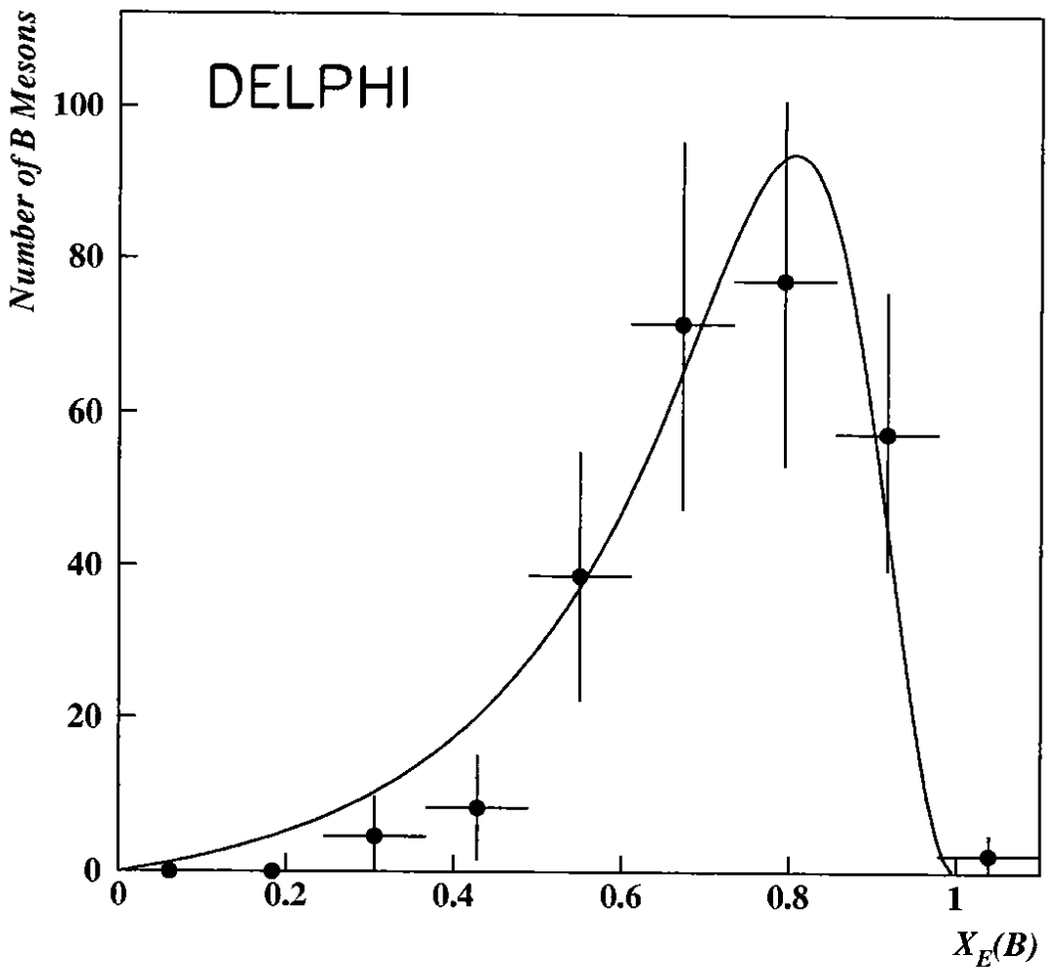

Figure 8:

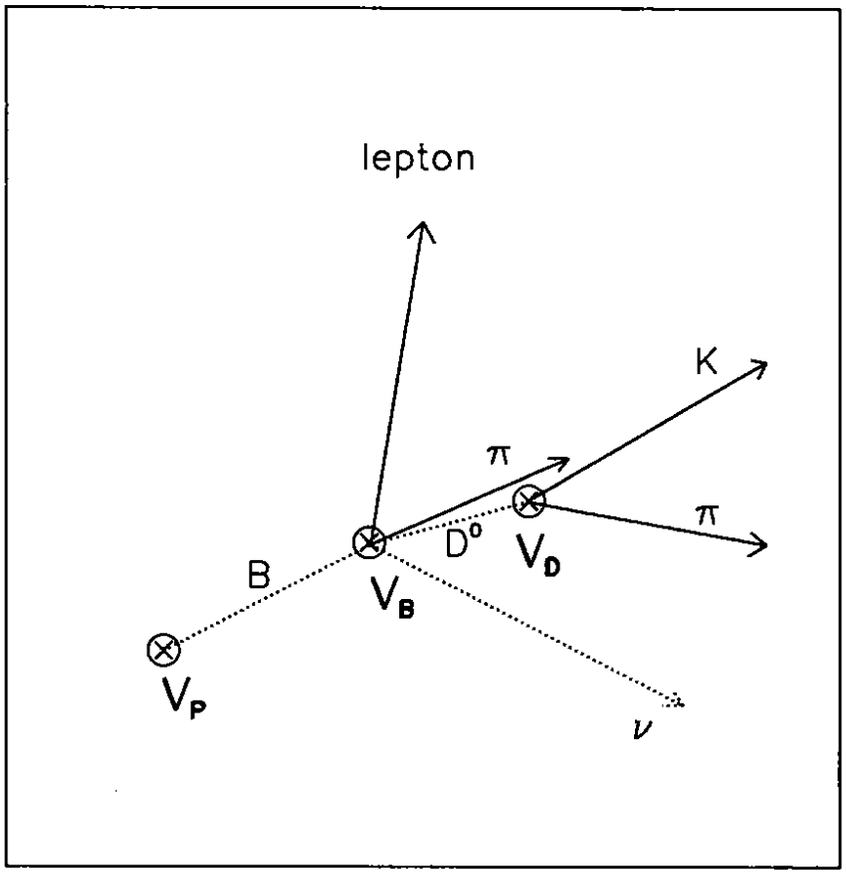

Figure 9:

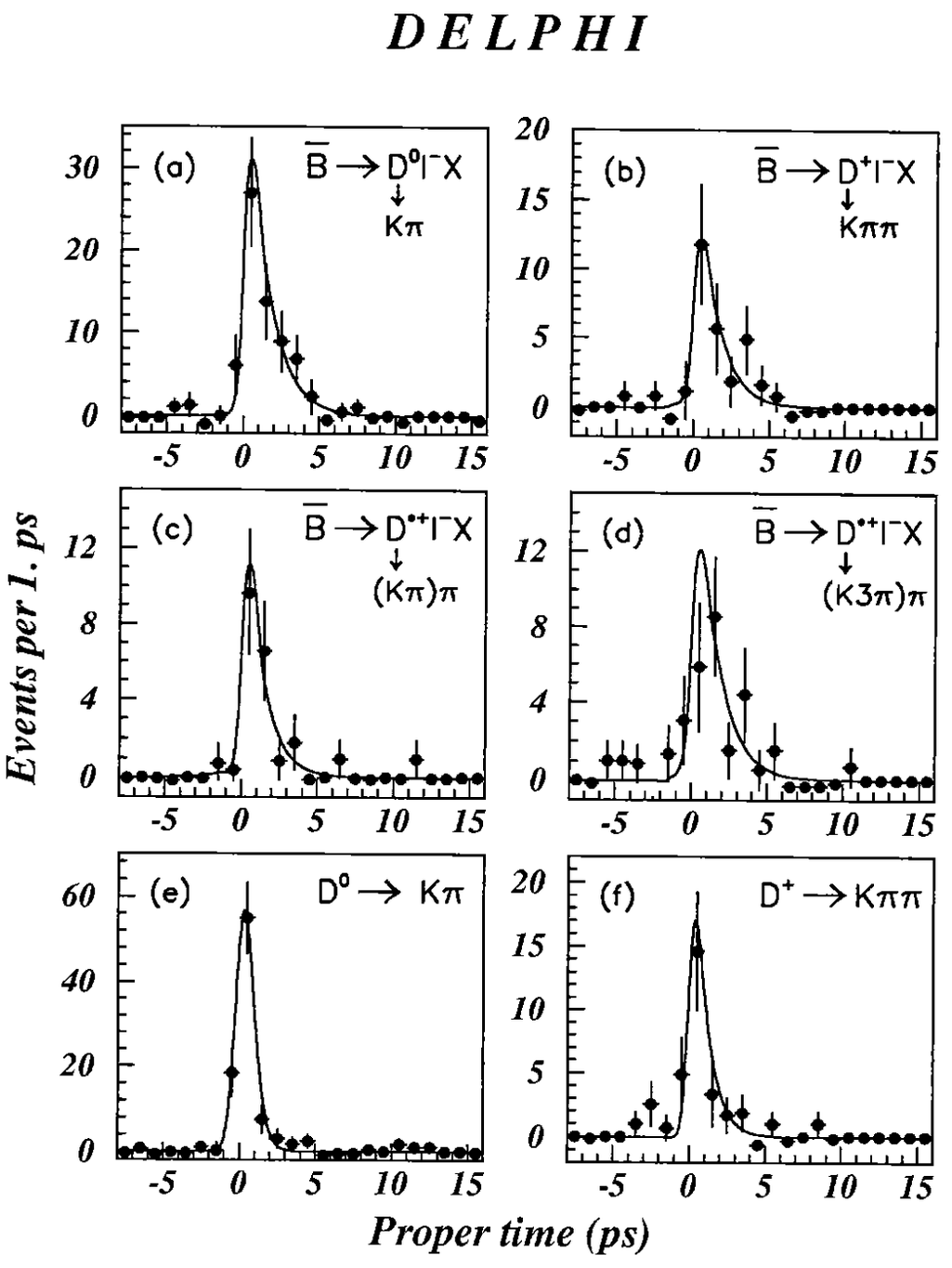
DELPHI
(a) $\bar{B} \to D^0 l^- X$ ↓ Kπ
(b) $\bar{B} \to D^+ l^- X$ ↓ Kππ
(c) $\bar{B} \to D^{*+} l^- X$ ↓ (Kπ)π
(d) $\bar{B} \to D^{*+} l^- X$ ↓ (K3π)π
(e) $D^0 \to K\pi$
(f) $D^+ \to K\pi\pi$
Events per 1. ps
Proper time (ps)

Figure 10:

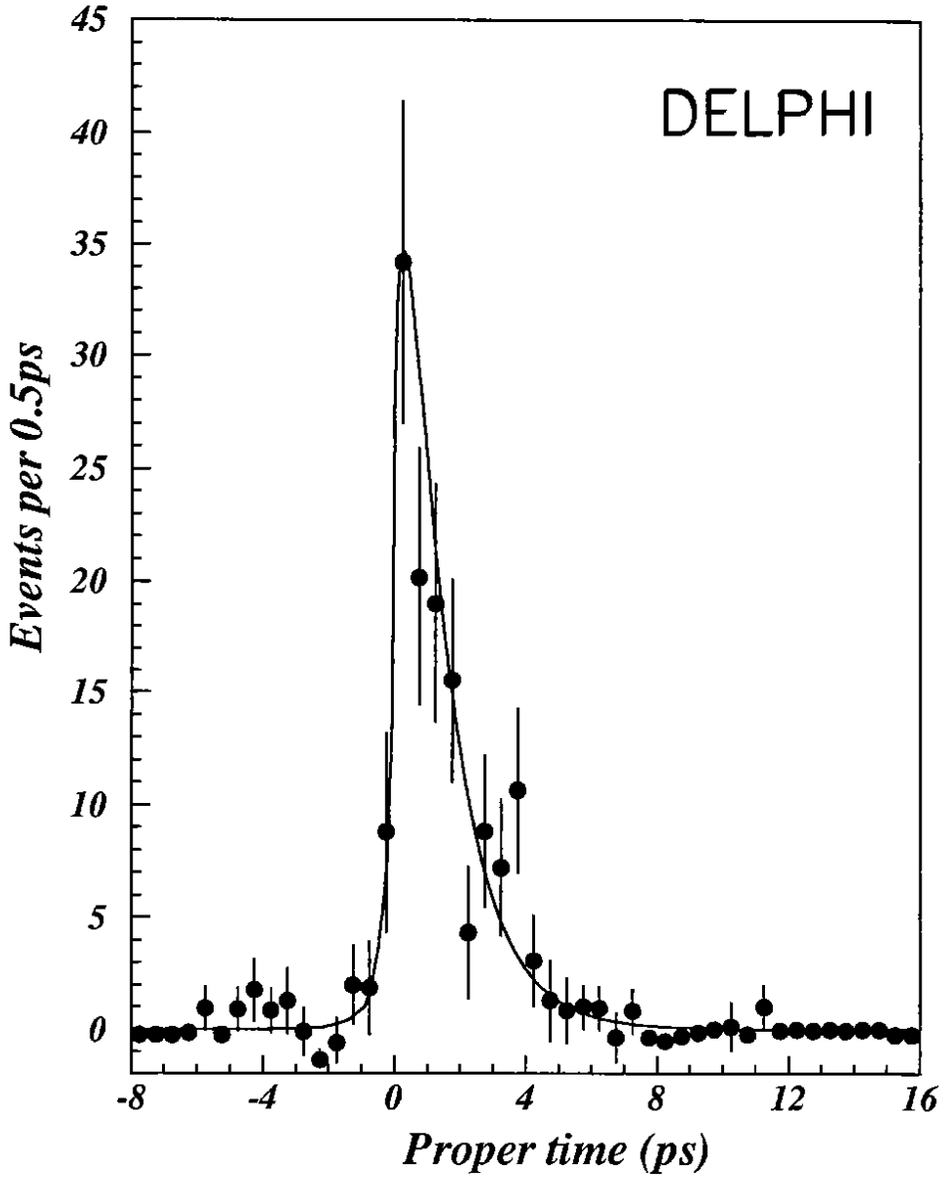
DELPHI
Events per 0.5ps
Proper time (ps)
45
40
35
30
25
20
15
10
5
0
-8
-4
0
4
8
12
16

Figure 11: